Investigation of the Mass-Metallicity Relation of GRB Host Galaxies at z ~ 4.7

A thesis presented to

the faculty of

the College of Arts and Sciences of Ohio University

In partial fulfillment

of the requirements for the degree

Master of Science

Huei M. Sears

December 2020

This thesis titled

Investigation of the Mass-Metallicity Relation of GRB Host Galaxies at z ~ 4.7

by

HUEI M. SEARS

has been approved for

the Department of Physics and Astronomy

and the College of Arts and Sciences by

Ryan Chornock

Assistant Professor, Physics and Astronomy

Florenz Plassmann

Dean, College of Arts and Science

Abstract

SEARS, HUEI M., M.S., December 2020, Physics

Investigation of the Mass-Metallicity Relation of GRB Host Galaxies at z ~ 4.7 (56 pp.)

Director of Thesis: Ryan Chornock

In studying the chemical abundance evolution of star-forming galaxies across many cosmic epochs, we will be able to understand how the chemical abundance of the Milky Way came to be. Determining chemical abundances (often generalized as "the metallicity") of galaxies is relatively straight forward to do but can become difficult at high redshift (z). Gamma-Ray Bursts (GRBs) offer a unique way to spectroscopically view high redshift galaxies. Before GRBs can be confidently used as probes of the high-redshift star-forming universe, it must be first determined if GRBs trace star formation.

In the local universe, it has been shown that GRBs prefer metal-poor environments and this preference does not evolve much with redshift. On the other hand, the Mass-Metallicity (M-Z) relation of star-forming galaxies evolves toward lower metallicities with increasing redshift. It is theorized that after $z \sim 3$, GRBs should be unbiased tracers of star-formation and could be used as probes of otherwise unobservable aspects of the high redshift universe.

Presented here is the analysis of a sample of 11 GRB host galaxies at redshift $z \sim 4.7$. Though the larger project consists of a sample of 23 GRB host galaxies, at this time, only 11 had sufficient data for analysis. Analysis of the remaining 12 galaxies in the sample is ongoing. *Spitzer Space Telescope* images exist for all 23 hosts, while *Hubble Space Telescope* (HST) images were taken of 19 of the hosts over the last two years. Archival HST images will be used for the remaining four galaxies. Masses and metallicities for these 11 hosts were collected from the literature. Metallicities were converted to gas-phase oxygen abundances for comparison to M-Z relations of star-forming galaxies. Our collaborators measured observed-frame Infrared (IR) magnitudes for 5 of the galaxies

in our sample, though further analysis for the remaining sample is ongoing. These magnitudes were converted to masses using a mass-to-light ratio for star-forming galaxies at $z \sim 4$. Despite theoretical prediction that GRBs should be unbiased tracers of star-formation after $z \sim 3$, we find that even at $z \sim 4.7$, GRBs prefer metal-poor host galaxies. The offset from the closest M-Z relation at $z \sim 3.5$ is on the order of 1 dex. There does seem to be some agreement with our sample and the M-Z relation of star-forming galaxies at $z \sim 8$, though further analysis is necessary due to the large scatter of the relation and incomplete GRB host sample.

DEDICATION

I dedicate this to my parents and two sisters, Lou and Francis.

Acknowledgments

Results presented within this thesis are based on observations made with the NASA/ESA Hubble Space Telescope, obtained at the Space Telescope Science Institute, which is operated by the Association of Universities for Research in Astronomy, Inc., under NASA contract NAS5-26555. These observations are associated with program GO-15644. Figures and data calculations were completed using *matplotlib* ([40]), *numpy* ([90], [68]), *jupyter* ([47]), & *python* ([91]).

Table of Contents

List of Tables

List of Figures

1 What are Gamma-Ray Bursts?

1.1 What is a Gamma-Ray Burst?

A Gamma-Ray Burst (GRB) is, as its name suggests, a sudden burst of gamma-rays in an otherwise dim/dark gamma-ray sky. Initially discovered in 1969 with nuclear weapon detecting military satellites (Klebesadel et al. [46]), gamma-ray bursts have been a highly-energetic source of interest for decades. They come in two main types: short (gamma-ray prompt emission < 2s) and long (gamma-ray prompt emission > 2s). This separation based on prompt emission length is supported by an anti-correlation with gamma-ray spectrum hardness (Dezalay et al. [25], Kouveliotou et al. [49]). Additionally, this classification is supported by evidence for different progenitor pathways. Long GRBs are known to be created from the deaths of massive stars and are usually associated with Type Ic-bl supernovae (SNe) (see Galama et al. [29] and Hjorth and Bloom [38]). Short GRBs, on the other hand, have been thought to be created from neutron star binary mergers or neutron star – black hole mergers (Nakar [67], Berger et al. [8], Tanvir et al. [85]), but evidence for this path of creation was not provided until the observation of GRB 170817A concurrent with the binary neutron star merger GW170817 (Abbott et al. [2]). Unless otherwise indicated, all GRBs mentioned further are long GRBs.

1.2 How is a GRB formed?

Statistical studies showing the correlation between the blue light of GRB host galaxies and the location of the GRB strongly suggest that GRBs occur in regions where the most massive stars die. GRB occur in smaller, dimmer, and more irregular galaxies than standard star-forming galaxies at similar redshifts. There is spectroscopic evidence that GRBs are associated with active star-forming regions within their hosts. (Woosley and Bloom [94], section 2.1.2 and references therein.)

As is common with the deaths of massive stars, there is usually a supernova (SN) component to the deaths of the stars that create GRBs. Though supernovae (SNe) come in many types, all SNe associated with GRBs are Type Ic-bl. Type I SNe have no hydrogen emission lines in their spectrum, and Type Ic additionally have neither helium nor silicon lines. There is also a distinction between the pathway to explosion between the types of SNe; Type Ia SNe are sometimes referred to as "Thermonuclear SNe", while all other types are referred to as "core collapse SNe." Some Type Ic SNe have very broad emission lines (which are indicative of quickly expanding material); these are called "Type Ic-bl" SNe, where the "bl" stands for "broad line" (Branch and Wheeler [11]).

The first GRB to be formally associated with a SN was GRB 980425. Although sub-luminous, this GRB is notable for its close proximity of z = 0.0087. The supernova, SN 1998bw, was identified as a Type Ic-bl due to its lack of H and He I lines and broad P Cygni features. Though the GRB-SN connection was debated for this case, identification of a variable X-ray source associated with the SN confirmed that GRB 980425 and SN 1998bw were from the same object (Kouveliotou et al. [50]). Since 1998, several other SN have been identified with GRBs; some well studied examples are GRB 030329/SN 2003dh (Matheson et al. [63]), GRB 111209A/SN 2011kl (Greiner et al. [36]), GRB 120422A/SN 2012bz (Schulze et al. [80]), and GRB 130702A/SN 2013dx (Toy et al. [88]); all have been Type Ic-bl SNe. It's important to note that although all GRBs have an associated Type Ic-bl SNe, the reverse cannot be said. This inequality is an active area of research (Japelj et al. [41]).

The collapsing star "collapsar" method of GRB creation is one of the leading theories (MacFadyen and Woosley [59]), though other avenues to a GRB are being explored. In this avenue, a massive star collapses (hence the moniker "collapsar"), experiences a supernova explosion and forms a compact object (a black hole or neutron star). Another prominent theory is the "binary star model" (Chrimes et al. [17], Metha and Trenti [66]).

In this model the two stars maintain their angular momentum (as is needed for the jet production) while still losing their outer layers via stellar winds.

The process starts with a massive star that has evolved to no longer have a hydrogen or helium layer. Because the star is sufficiently massive, once the star starts to fuse iron, the iron core collapses into a stellar mass black hole. The surrounding inner layers collapse into an accretion disc around the black hole. The intense and complicated magnetic fields of the black hole cause jets to form, and within these jets, matter is ejected at relativistic speeds spiralling along the magnetic axis of the black hole. The jet continues outward through the star, speeding up as the density of the star decreases until finally reaching peak velocity at the surface of the star (MacFadyen and Woosley [59]). This initial burst of gamma-rays from the jet is what is considered to be the "prompt emission" of the GRB. As the jet continues through space, it eventually interacts with the interstellar medium (ISM). The resulting, less-energetic radiation from the interaction of the jet and ISM is what is referred to as the "afterglow" of the GRB (Gehrels et al. [30]).

2 How are GRBs Observed?

2.1 Pre-*Swift*

Since their discovery in 1969, GRBs have been intensely studied. One of the first space-based telescopes dedicated to their study was the Arthur Holly Compton Gamma Ray Observatory (abbreviated "Compton" or CGRO) launched in 1991. Onboard this observatory were four instruments dedicated to covering energies between 0.1 MeV - 30 GeV. The instrument most helpful to GRB studies was the the Burst and Transient Source Experiment (BATSE) which collected data on the distribution of GRBs, the direction of sources, the location of general bursts, and fluctuations on time scales of 1 ms.[1] The first catalogue of BATSE observed GRBs was published in 2000 in Preece et al. [72]. Until its deorbit and crash landing back on Earth in 2000, CGRO was our foremost way of observing GRBs.

2.2 *Swift* Era

Launched in 2004, The Neil Gehrels Swift Observatory (Swift) has been finding GRBs with three instruments onboard. The first instrument used when detecting a gamma-ray burst is the "Burst Alert Telescope" (BAT). This instrument is sensitive to photons with energies between 15–150 keV and has arcminute accuracy. Five seconds after detecting a GRB, an alert is sent to astronomers on the ground through the Gamma-Ray Coordinates Network (GCN). Swift then centers the second instrument, the X-Ray Telescope (XRT), at the BAT-found location and takes an image. X-ray detectors read out each photon individually; this allows the energy of each photon to be measured and thus X-ray imaging naturally also provides a spectrum with each photometric image. XRT is sensitive to photons with energies of 0.3–10 keV and has an angular resolution of 1–3 arcseconds. This angular resolution is enough to sufficiently constrain the location of

[1] https://nssdc.gsfc.nasa.gov/nmc/experiment/display.action?id=1991-027B-05

the GRB for the third and final instrument, the UV/Optical Telescope (UVOT). The images from UVOT are then used to constrain the location of the burst to 0.5 arcsecond accuracy (Barthelmy et al. [6]). Astronomers on the ground can then complete follow-up observations with this new location. The planned mission length for Swift was 2 years, but the observatory has been successful for the last 15.

Though Swift was designed for GRB detection and is well regarded as the solar system's foremost GRB observatory, several other observatories have gamma-ray detectors that are used for GRB science. One prominent telescope is the Fermi Gamma-Ray Space Telescope (Fermi, but formerly GLAST). One of Fermi's main mission goals is to "determine the high-energy behavior of GRBs" [2]. On-board Fermi are two instruments: the Large Area Telescope (LAT) [3] and the GLAST Burst Monitor (GBM) [4]. With a field-of-view (FOV) of 2.4 sr (~ 1/5 of the sky) and an energy sensitivity of ~20 MeV – 300 GeV, LAT surveys the entire gamma-ray sky about every 3 hours. In complement, the GBM has a lower energy sensitivity (~10 keV – 25 MeV) and a much higher FOV (>8 sr) than LAT. In addition to providing the low-energy complement to the gamma-ray sky survey, GBM has a trigger on board that can localize a GRB location to within a few degrees. When there is an alert and when logistically possible, GBM signals to LAT to center on the GRB location for high-energy observation. This burst alert and other identifying information about the GRB is sent to the ground for further study. Although Fermi was launched in 2008 and had a five-year mission lifetime, it is still taking usable data more than a decade after its launch. Many space-based observatories or satellites have gamma-ray detectors on board used to help locate GRBs. Ones that do are part of the Interplanetary Network; this network includes Mars Odyssey, KONOS-Wind,

[2] https://www.nasa.gov/pdf/221503main_GLAST-041508.pdf

[3] https://fermi.gsfc.nasa.gov/ssc/data/analysis/documentation/Cicerone/Cicerone_Introduction/LAT_overview.html

[4] https://fermi.gsfc.nasa.gov/ssc/data/analysis/documentation/Cicerone/Cicerone_Introduction/GBM_overview.html

Swift, Fermi, and INTEGRAL, among many others.[5] INTEGRAL is the INTErnational Gamma-Ray Astrophysics Laboratory and was launched by the ESA in 2002. Though not designed to study GRBs, the large FOV of the main instruments allows INTEGRAL to detect a GRB every 1–2 months. A GRB detection sparks the INTEGRAL Burst Alert System (IBAS) which then sends energy and location information to astronomers on Earth.[6]

When observing GRBs, it is prudent to have quick follow-up, as the afterglow fades out of the optical/IR within a few hours after the initial burst of gamma-rays. This necessity for rapid response observations led to the creation of the Gamma-Ray Burst Coordinates Network (GCN). Observations from Swift, among other space-based observatories, are sent to this network, and ground-based astronomers can share their own observations of the afterglow to this network through GCN Circulars.

Spectroscopy is commonly of highest interest when studying the afterglow, though when the GRB is too faint, photometry can also be useful, especially for determining an otherwise indeterminable redshift. Because of the broad wavelength coverage of the afterglow, there are many observatories that can contribute to afterglow observations. ESO's Gamma-Ray Burst Optical/Near-IR Detector (GROND), located at La Silla Observatory, is one such instrument that is linked to autonomously do follow-up photometry on Swift burst alerts.[7]

2.3 Post-*Swift* Plans

Planned for launch in 2021, the upcoming Chinese-French Space Variable Objects Monitor (SVOM) will focus on using GRBs to study massive stars. This small telescope does much of the same as Swift but has an enhanced gamma-ray spectrometer that makes

[5] https://heasarc.gsfc.nasa.gov/W3Browse/all/ipngrb.html
[6] http://ibas.iasf-milano.inaf.it/
[7] https://www.eso.org/public/teles-instr/lasilla/mpg22/grond/

it more sensitive to high-redshift GRBs. In addition to a space-based x-ray satellite, there are planned to be three ground-based telescopes used for surveying the sky pre-GRB and used for follow-up visual observations (Wei et al. [93]).

2.4 Science Determination

When possible, the redshift of the gamma-ray burst is determined spectroscopically. Following the burst alert from Swift, ground follow-up observations are taken. Although there is a an optical spectrometer on Swift, it is not as sensitive as those that are on the ground. Astronomers then look for narrow absorption lines in the continuum spectrum from the synchotron radiation. A confident redshift determination is usually made from an agreement between several absorption lines.

When the GRB is too faint for a spectroscopic redshift determination, other methods are used. Most common is using spectral energy distribution (SED) fitting to constrain a photometric redshift. This way of determining GRB redshifts is quick, as it can be done from the photometric images from Swift taken minutes after the initial BAT alert, but is not without its faults. Due to the nature of the method and the faintness of the source GRBs, redshifts determined in this way are at best lower limits.

2.5 What is Metallicity?

In astronomy, a metal is often considered to be any element heavier than hydrogen or helium. The "metallicity" of a source (be it a star or galaxy) is always a ratio, of some sort, of the metal content of the source to the hydrogen or helium content of the source; this is usually denoted with a capital Z (not to be confused with cosmological redshift which is symbolized with a lowercase z). A common way to represent the metallicity of a source with a logarithmic comparison to the solar metal abundance symbolized by "[M/H]" where:

$$[M/H] = \log_{10}((M/H)/(M/H)_\odot) \tag{2.1}$$

and "M" is a placeholder for whatever element(s) may be of most interest. Solar metal abundances are updated every several years; the most up to date reference for these values is Asplund et al. [5]. Metal abundances for galaxies can be determined in a multitude of ways, though this becomes difficult with faint sources. Metal abundances for low redshift galaxies are often determined using the "strong-line" or "emission-line" method. Metal and hydrogen emission line strength is determined from a spectrum of the source. Lines of interest are fit with a Gaussian (or other type of Voit profile); the peak fluxes of these lines are the values then used in the (M/H) ratios. Hydrogen strength is usually determined from the Hβ lines, while the metal strength can be determined from a variety of lines. This method faces faults: calibration values are set in the very local universe and don't always properly translate to the less local universe; additionally some of the most preferred metal ratios for this method can be double valued - namely those featuring the [OIII] and [OII] lines at $\lambda\lambda 4959, 5007$ + $\lambda\lambda 3726, 3729$, respectively. This method and its faults are outlined well in Sanders et al. [77].

Though the strong-line method is preferred, it is not always possible to determine galactic metallicities in that way. Specifically, when galaxies are too faint, it can be difficult to near-impossible to get a sufficiently strong spectrum to use this method. This is where GRBs really shine. GRBs act like a back light to an otherwise too-dim-to-observe galaxy. With some assumptions about metallicity distribution within the host galaxy and generalizations of GRB lines-of-sight through the host, galactic metallicities can be determined from the absorption lines in a GRB's afterglow spectrum. Obtaining metallicities from an absorption spectrum is very similar to that of an emission spectrum; the fits are just troughs instead of peaks. The fits from these absorption lines are then converted to "equivalent widths (EWs)." An "equivalent width" of a line is the width of a rectangle under the continuum (in this case, the black-body spectrum of the galaxy) whose area is the same as that under the Voit profile. These EWs are then converted to column densities which are the values used in the (M/H) ratios. This method is explained in more detail in de Ugarte Postigo et al. [24] and Chornock et al. [16].

Another form of metallicity that is seen is the gas-phase oxygen abundance which is commonly reported as $12 + \log_{10}(O/H)$. It is straightforward to go between the two standard metallicity "units" as:

$$[M/H] = \log_{10}((M/H)/(M/H)_{\odot}) \tag{2.2}$$

$$= \log_{10}(M/H) - \log_{10}(M/H)_{\odot} - 12 + 12 \tag{2.3}$$

$$12 + \log_{10}(M/H) = \log_{10}(M/H)_{\odot} + 12 + [M/H] \tag{2.4}$$

Translations between abundances of individual elements (i.e., [M/H] to [O/H]) can be complicated and require further knowledge about the expected abundance ratios in the galaxy. As a first approximation, to get $12 + \log_{10}(O/H)$ metallicity values, it is often assumed that all gas-phase metal abundances of the host are equal to the gas-phase oxygen abundance (i.e., $[M/H] = [O/H]$).

3 What Has Been Done?

3.1 Why Do We Care

We are interested in studying the mass-metallicity (MZ or M-Z) relation, especially at high redshift, because we are interested in the history of the Milky Way. Research has been done into the metal content and distribution within our host galaxy (McWilliam [65], Tinsley [87]), and it's important to study similar characteristics in galaxies that will one day form into a galaxy like ours. The mass-metallicity relation, by nature, is a an indicator of the metal distribution of large galaxy samples. We know that with time galaxies grow in stellar mass and so comparing the mass-metallicity relations over redshift allow us to characterize the (possibly) changing metal content of star-forming galaxies.

We are interested in using GRB host galaxies to probe this relation because our current methods of measuring metallicities at high redshift are lacking. Galaxies at high redshift are often too faint to directly observe which leaves survey studies with low number statistics and high uncertainties on fits. New space-based telescopes, like the James Webb Space Telescope (JWST), will have capabilities that make observation of faint objects possible, but it's important to visit other options to have an independent check on the results from JWST. As detailed below, galaxy surveys in the local universe ($z \sim 0.1$) have hundreds of thousands of galaxies to find MZ relation fits to, while in the further universe, ($z \sim 3$) galaxy surveys struggle to get above 20 suitable spectra for metallicity analysis. As covered in Chapters 1 and 2, GRBs offer a unique opportunity to study otherwise unlit galaxies. These GRBs act as a lighthouse, of sorts, illuminating the intergalactic medium of their host galaxies across the electromagnetic spectrum. GRBs have shown to originate from the deaths of massive stars and should then therefore be an indicator of the SFR of their host galaxy. If GRB host galaxies prove to follow the same trends as field star-forming galaxies, GRB afterglow spectroscopy can be a helpful tool in studying high-redshift star-forming galaxies.

The goal for our project is to use GRB host galaxies at $z \sim 4.7$ to probe the mass-metallicity relation of star-forming galaxies. In the sections below is a literature review of what's known about the MZ relation of star-forming galaxies and what's known about the MZ relation of GRB host galaxies.

3.2 General Star-Forming Galaxies

In order to confidently use GRBs as tracers of star-formation at high-redshift, we must first understand how GRBs and star-formation are linked in the local universe. One of the first studies on the mass-metallicity relation of local star-forming galaxies was completed by Tremonti et al. [89]. This team looked at $\sim 53,000$ star-forming galaxies at $z \sim 0.1$ and found a tight correlation (± 0.1 dex) between their mass and metallicity. Shown in Fig 3.1, they were able to fit a second-order polynomial to the data and found it to be valid over the mass range $8.5 < \log_{10}(M_*/M_\odot) < 11.5$. They note that this relation is roughly linear until $\log_{10}(M_*/M_\odot) = 10.5$ after which it then flattens out at $12 + \log_{10}(O/H) = 9.1$. This paper was notable because it was one of the first papers to combine the statistical power of a large survey like the Sloan Digital Sky Survey (SDSS) with improved techniques to measure the mass and metallicity (Kauffmann et al. [44], Charlot and Longhetti [13]).

Following the success from the Tremonti et al. [89], the study of the mass-metallicity relation continued onward to higher redshifts. Published in 2006, Erb et al. [26] secured a mass-metallicity relation at $z \sim 2.26$. This relation was fit from 87 rest-frame UV-selected star-forming galaxies. They find that mass and metallicity are still tightly correlated and that the relation has roughly the same shape as that from Tremonti et al. [89], but that the relation is shifted toward lower metallicities by ~ 0.3 dex. This offset gets smaller with

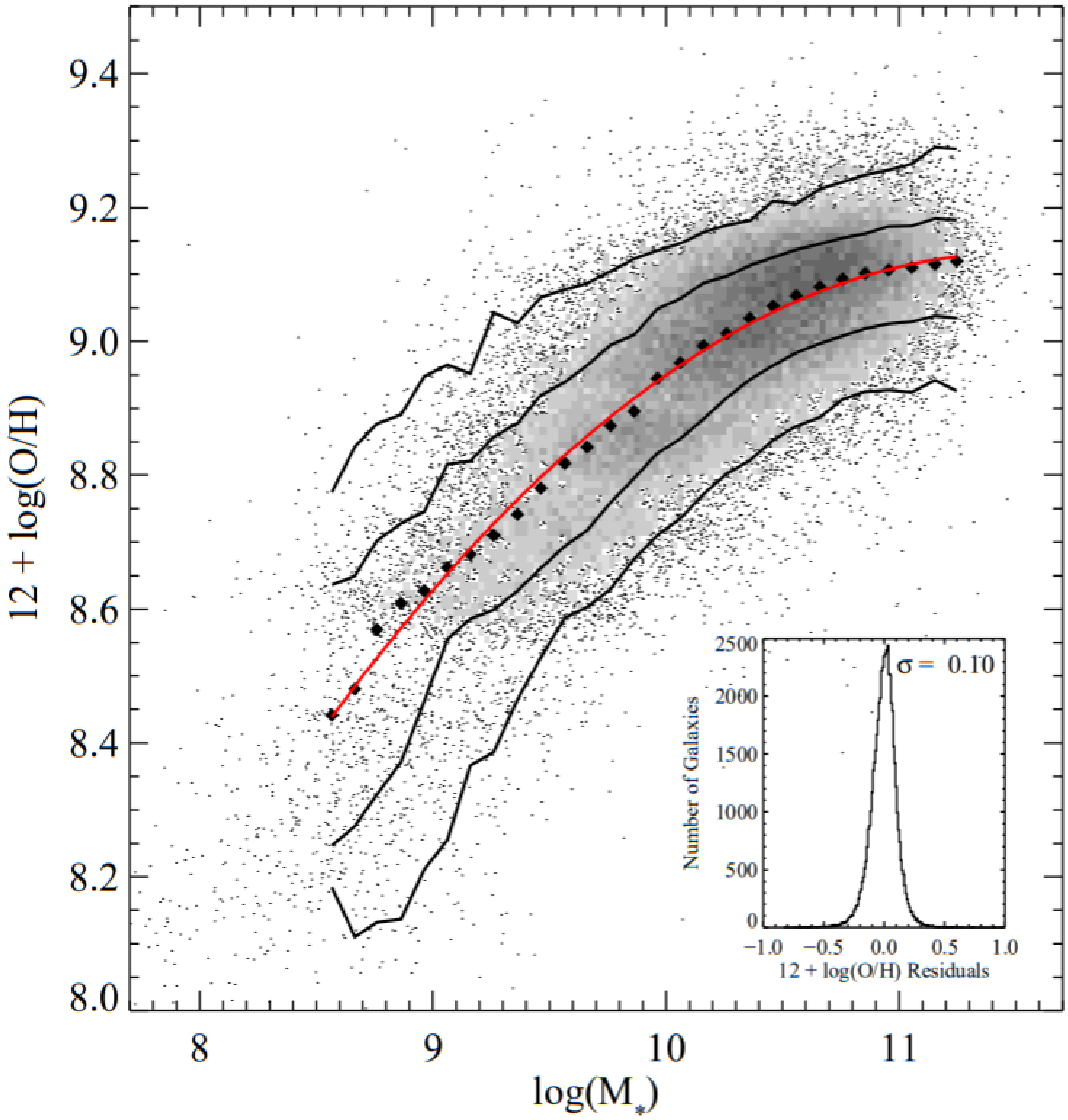

Figure 3.1: The mass-metallicity relation of $\sim 53,000$ star-forming galaxies at $z \sim 0$ from the Sloan Digital Sky Survey (SDSS). The large black points represent the median values for 0.1 dex mass bins of galaxies. The solid black lines show contours for 65% and 98% of the data, while the red solid line shows the best fit to the presented data. The inset plot shows the residuals of the fit. This figure is reproduced from Tremonti et al. [89] by permission of the AAS. © AAS.

higher masses (above $\log_{10}(M_*/M_\odot) = 10.5$) due to the higher-redshift galaxies not reaching the saturation metallicity at the same mass as the low-redshift sample. Similar findings of the MZ relation having the same shape but offset toward lower metallicity were shown at $z \sim 0.35$ (Lara-López et al. [54], Lara-López et al. [55], offset by -0.1 dex), $z \sim 0.6$ (Rodrigues et al. [74], offset by -0.3 dex), and at $z \sim 3.5$ (Maiolino et al. [60], decreased in metallicity by a factor of 2.5 from the $z \sim 2.2$ sample).

In 2010, Mannucci et al. [61] further investigated the low redshift ($z = 0.07 - 0.3$) star-forming universe and found that the observed mass-metallicity relation was actually a consequence of a larger relation between mass, metallicity, and the star-formation rate. Fit to ~140,000 SDSS galaxies, this so called "fundamental metallicity relation" (FMR) has a scatter of only 0.05 dex (~ 12%) in metallicity. At galaxies with low mass, they find that metallicity and star-formation are sharply anti-correlated while at high mass there is no SFR-Z relation. Mannucci et al. further find that, up to $z = 2.5$, there is no evolution in the FMR and that the observed tendency in the MZ relation toward lower metallicity (at a given mass) is a consequence of viewing galaxies with higher star-formation. After $z = 2.5$, there is an evolution of 0.6 dex in the FMR toward lower metallicity. Around this same time, the team from Lara-López et al. [56] also independently discovered a M_*-Z-SFR relation fit from 34,575 field galaxies. Much later in 2018, A M-SFR-Z relation for field galaxies at $z \sim 2.3$ was published in Sanders et al. [76]. This relation is shown in Figure 3.2. They find that at $z \sim 2.3$, galaxies with a fixed stellar mass and SFR have 0.1 dex lower metallicity than the $z \sim 0$ sample from Andrews and Martini [4].

In 2012, Yabe et al. [95] characterized the MZ relation at $z \sim 1.4$. They found that it lies between those found in Tremonti et al. [89] and Erb et al. [26], with an average scatter of only 0.1 dex. They also find that this mass-metallicity relation is dependent on the SFR: at constant mass, galaxies with a higher SFR show lower metallicities. In comparison with simulations and fitted relations, they find that the mass-metallicity relation evolves smoothly without much shape change between redshifts $z = 0$ and $z = 3$, save for the metallicity saturation of the $z = 0$ sample. Furthermore they find that they can characterize

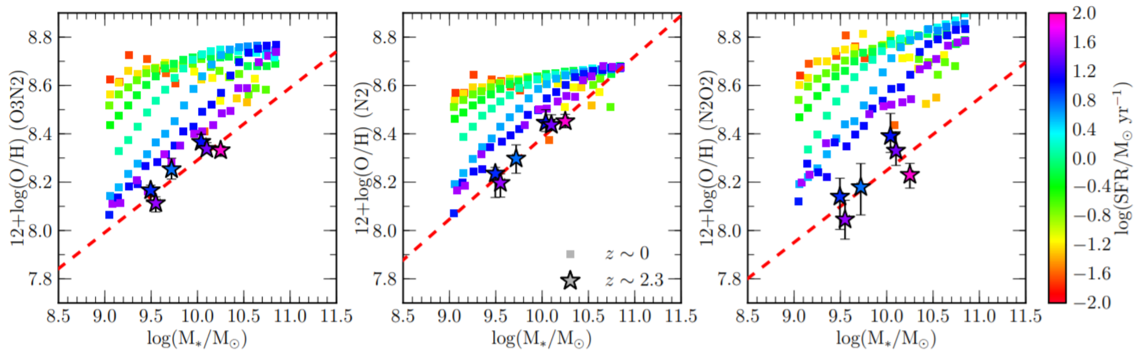

Figure 3.2: Shown here are the mass-metallicity relations from stacks at z ∼ 0 (squares) and $z \sim 2.3$ (stars) color-coded by SFR. The red-dashed line shows the best mass-metallicity relation fit for the z∼ 2.3 sample. The three plots show different methods of metallicity estimation (i.e. the left-most plot presents the data when the O3N2 line-ratio were used for metallicity calculation). O3N2 = O3/N2, N2 = [NII]λ6584/Hα, and N2O2 = [NII]λ6584/[OII]$\lambda\lambda$3726, 3729. This figure is reproduced from Sanders et al. [76] by permission of the AAS. © AAS.

the metallicity around this "tipping point" of $\log_{10}(M_*/M_\odot) = 10$ by a polynomial of order 1.3 in redshift.

Zahid et al. [97] further characterized the MZ relation by presenting relations at 5 epochs up to $z = 2.3$. Data for their first three redshift bins was collected from SDSS DR7 (Abazajian et al. [1]), SHELS (Geller et al. [31]), and DEEP2 (Davis et al. [22]), while the data for the final two bins was taken from Erb et al. [26] and Yabe et al. [95]. In comparing these five relations, they report similar findings to what has already been said, namely that there is an evolution toward lower metallicities with increasing redshift at a constant mass. Unlike earlier publications, though, they qualify the slight changing in shape of the relations at redshifts less that $z = 0.8$. They claim that this shape evolution is due to non-evolving upper-limit on the gas-phase oxygen abundance of star-forming galaxies.

Most recently in 2020, Jones et al. [43] established a mass-metallicity relation at $z \sim 8$ and found it to be of a similar shape to that of Tremonti et al. [89] but just shifted down in metallicity by 0.9 dex. Also in 2020, Curti et al. [20] revisited the FMR discovered in Mannucci et al. [61] and recalculated it using a more sensitive and consistent metallicity method.

There has been a strong relation between mass and metallicity up the highest redshifts, and though the relation shifts toward lower metallicities with increasing redshift, the overall shape of the relation does not change much. Below redshift $z \sim 0.8$, this relation flattens in galaxies with masses $\log_{10}(M_*/M_\odot) > 10$ to a metallicity around the solar gas-phase oxygen abundance. Furthermore, it has been shown that up to $z \sim 2.5$, the mass-metallicity relation is a consequence of a larger, non-evolving M-Z-SFR relation. This M-Z-SFR relation has been shown to evolve toward lower metallicities after $z \sim 2.5$.

3.3 GRB Science

Concurrent with research on characterizing field galaxies, astronomers also needed to characterize GRB host galaxies. Although it is well established now that GRBs prefer metal-poor environments, the first mention of a metal-aversion was in 2006 by Stanek et al. [83]. In this study, they looked at 5 local GRBs ($z < 0.25$) and they compared them to large samples (N > 73,000) of local field galaxies (Tremonti et al. [89], Kauffmann et al. [45], Brinchmann et al. [12]). In study of the field comparison samples, they found that less than 25% of star-formation happens in field galaxies with metallicities, $12 + \log_{10}(O/H) \leq 8.6$. Their five (5) local GRBs had metallicities ranging 7.9 - 8.6. They found that the probability of this GRB metallicity distribution occurring if GRBs were unbiased tracers of star-formation to be less than 0.1% and therefore conclude that GRBs do not trace local star-formation.

In support of Stanek et al. [83]'s conclusion, studies were done on GRB hosts up to $z = 1$. Han et al. [37] collected 8 GRBs with redshifts less than 1. The immediate goal of their project was to determine if Wolf-Rayet (WR) stars were observable in the GRB host galaxies, though they also wanted to investigate the $L_* - M$ and $M - Z$ relations of the galaxies. They found WR stars in 5 of the 8 host galaxies and found that, when compared to non-GRB host star-forming galaxies at comparable luminosity and mass, GRB hosts have metal-poor environments. The first large GRB host survey was published in 2010 by Levesque et al. [58]. This paper established a mass-metallicity relation for 16 GRB hosts up to redshift z = 1. In comparison with mass-metallicity relations for standard star-forming galaxies (Tremonti et al. [89] for $z < 0.3$ and Zahid et al. [96] for $0.3 < z < 1$), the M-Z relation for GRB hosts was on average offset in metallicity by -0.42 ± 0.18 dex. Further comparison to a $z \geq 2$ field galaxy sample (Erb et al. [26]) showed a smaller offset and suggested that GRBs may be tracers of general star-forming galaxies at higher redshifts.

Moving on to higher redshifts, a *Spitzer* campaign was completed focused on GRB host galaxies with redshift $z = 2 - 5$. Laskar et al. [57] focused on the $z = 3 - 5$ sample of this campaign. In their paper, this team separated their sample of 18 GRB host galaxies into two mass bins ($2 * 10^{10} M_{\odot}$ and $< 3 * 10^{9} M_{\odot}$) and found that the average metallicity decreased by a factor of 10 with decreasing mass. This trend is indicative of a GRB mass-metallicity relation. The authors also point out that the two mass-metallicity points lie below the M-Z relations at lower redshift and suggest that this could also be indicative of further redshift evolution of the M-Z relation. Also in 2011, Mannucci et al. [62] states that the previously discovered "Fundamental Metallicity Relation" (FMR) in general star-forming galaxies from Mannucci et al. [61] was also applicable to GRB host galaxies. This paper further claimed that the observed GRB metal aversion was a consequence of GRBs preferring low mass, high star-forming regions, as star-formation and metallicity are anti-correlated. This claim was later disproven in 2013 when Graham and Fruchter [33] compared the metallicities of galactic hosts of GRBs, Type Ic-bl SNe, and Type II SNe to the metallicity distribution of general star-forming galaxies. In these comparisons, they found that although $\sim 75\%$ of GRBs occur in hosts with metallicities,

$12 + \log_{10}(O/H) < 8.6$, less than 10% of star-formation happens below this metallicity. Furthermore, they found that the star-formation rate distributions of the host samples were consistent with that of the star-forming galaxies.

Following this discovery of the strong majority of GRBs occurring in galaxies with metallicities, $12 + \log_{10}(O/H) < 8.6$, research was launched into this metallicity barrier. The Swift Gamma-Ray Burst Host Galaxy Legacy Survey (SHOALS) claimed a near-solar metallicity ($12 + \log_{10}(O/H) \sim 8.7$) threshold for GRB host galaxies (Perley et al. [70], Perley et al. [71]). This survey was unique and ground breaking because of its commitment to producing the largest unbiased sample of GRB host galaxies. A similar, but smaller, endeavor was taken in Schulze et al. [79]. Detailed in the first SHOALS paper, GRB hosts were selected based on a number of qualifications, including, but not limited to, afterglow telescope location on Earth, lunar illumination at time of burst, and galactic extinction. Once the 119 GRB hosts were selected, they were then imaged with *Spitzer*. These images were supplemented by multicolor optical and near-IR photometry and spectroscopy. The second paper offered support for a near-solar metallicity threshold and detailed the rest-frame near-IR luminosity distribution. Along the lines of the second paper, Greiner et al. [35] showed that after redshift $z \sim 3$, GRB host galaxies have the same luminosity function as Lyman-break galaxies; this implies that after $z \sim 3$, GRBs should be unbiased tracers of star-formation.

More recently in 2019, this metallicity threshold was upheld with the publications of Palmerio et al. [69] and Graham et al. [34]. The paper by Palmerio et al. looked at a sample of 15 GRB host galaxies with redshifts between 1 and 2. Masses, SRFs, and metallicities were calculated for each of these galaxies for comparison to a general star-forming galaxy sample comprised of sources from COSMOS2015 (Laigle et al. [53]) and the MOSDEF Survey (Kriek et al. [51]). In this comparison, they found evolution in galaxy properties from $z < 1$ to $1 < z < 2$. Average SFR and mass both increase, while metallicity stays constant at $12 + \log_{10}(O/H) \sim 8.4 \pm 0.1$. They found a weaker than expected evolution in the SFR-M relation, which they say can be explained by a metallicity threshold. By comparing the cumulative distribution functions (CDFs) of mass, metallicity, SFR, and sSFR (SFR/M) to those of the comparison sample, they try to determine if GRBs are pure star-formation tracers. They find that the best explanation for the discrepancies between the mass and matallicity CDFs is a decrease in GRB production after $12 + \log_{10}(O/H) = 8.55$.

The paper by Graham et al. takes a different route in showing support for the metallicity threshold. They first formed a sample of GRB hosts out to $z \leq 2.5$. Redshift 2.5 was chosen because they were unable to collect metallicity measurements past that redshift. The sample is compiled from several other samples, and great care is taken into making sure their respective sample sizes are normalized. The find that there is no evolution in the metallicity distribution of GRB hosts up to $z = 2.5$, and more importantly they find that the fraction of GRB hosts with metallicities, $12 + \log_{10}(O/H) > 8.4$ is near constant to $z = 2.5$. Finally they compare estimated metallicities to 29 measured metallicities. They calculated these estimated metallicities from relations for star-forming galaxies in Zahid et al. [97]. They find a distinct separation; the est. metallicities are higher by about 0.25 dex. More data is needed to increase confidence in this offset as currently it is statistically random. That said, it suggests that there is no substitute for actually measuring GRB host metallicities.

There has been some work on GRB host galaxies past redshift $z \sim 6$. McGuire et al. [64] observed three GRB host galaxies at $z = 5.9 - 6.3$. This paper was notable because it was one of the first presentations of direct imaging for such high-redshift hosts. Broader implications of these GRB hosts are not discussed in this paper, but it is mentioned that from the afterglow spectra, all three have low metallicities. Tanvir et al. [84] present late-time HST imaging of 6 GRB host galaxies at $5 \leq z \leq 9.5$, but mention that they were only able to detect one of the six GRB hosts at $z = 8.11$. Based on the lack of detections, they concluded that since GRBs trace star-formation, much of the star-formation in this era occurs in small, faint galaxies. This conclusion relies on two central assumptions: 1. environmental conditions to not appreciably effect the SFR to GRB rate ratio and 2. dust content of the host galaxy is generally negligible. Since the publication of this paper in 2012, research has shown that the second assumption is not valid. Specifically, Perley et al. [71] found that the large majority of high-mass GRB hosts are dust obscured (and would this not have been detected in Tanvir et al. [84]'s survey).

In short, GRB host galaxies do not follow the mass-metallicity relation of star-forming galaxies. A MZ relation for GRB hosts has been established up to $z \sim 1$ and it has roughly the same shape as the relation for general star-forming galaxies, just shifted to 0.4 dex lower metallicity. This relation then stays constant to $z \sim 2.5$, as there has been shown to be no evolution in the metallicity distribution of GRB hosts to that redshift. A relation at $z = 3 - 5$ has been implied, but not yet characterized. There is a well established metallicity threshold of $12 + \log_{10}(O/H) \sim 8.7$, after which GRBs rarely occur. Because of this metal-aversion and the similarity of the low-z MZ relation of GRB host galaxies, it is implied that after $z \sim 3$, GRBs should be unbiased tracers of star-formation and more specifically, the GRB host MZ relation should be the same as that of general star-forming galaxies.

4 My Project

4.1 Project Motivation and Detail

As detailed in Chapter 3, much has been discovered about GRBs and their relation to the mass and metallicity of their host galaxy. Much of this work has been done on galaxies below redshift $z \sim 4$ (see Chapter 3) and above redshift $z \sim 6$ (McGuire et al. [64], Tanvir et al. [84], Chornock et al. [16]). There is a distinct lack of follow up on GRBs in this redshift window of $z = 4 - 6$; Of the near 30 GRBs detected by Swift in this redshift range, only a few have been followed up with HST.

We obtained images of 19 of the 23 GRB host galaxies in the sample with Hubble Space Telescope's (HST's) Wide Field Infrared Camera 3 (WFC3) using the F110W filter (a broad infrared filter with central wavelength 11,580 Å) over the past two years. The remaining four galaxies were previously imaged with WFC3 and archival data was used. The 23 GRBs were chosen based on redshift and were sourced from previous Cycle 9, 11, and 13 *Spitzer* large proposals. All GRBs within these proposals with redshifts $4 < z < 6$ were chosen for this project. The instrument and filter selected, WFC3-IR and F110W, were chosen for their wide coverage and high sensitivity. Filter F110W probes the rest-frame UV ($\sim$ 2000 Å), which is sensitive to the SFR of the host galaxy. Additionally, this is the only wavelength range at which there are complete samples of general star-forming galaxies, thereby making comparison only possible with rest-frame UV observations of out GRB host galaxies.

4.2 Data Conversion and Presentation

Over the past year, while the Hubble Space Telescope was taking the images, we collected information on a lower-redshift (z~2.5) sample of GRBs. This redshift window was selected to compare to the published MZ relation in Sanders et al. [76]. I selected GRBs that had masses published in Perley et al. [70] and then searched the literature for metallicites for those GRBs. I was only able to find published metallicites for six GRBs. These [M/H] metallicities were converted to gas-phase oxygen abundances, 12 + $\log_{10}(O/H)$, by first assuming $[O/H] = [M/H]$ and then calculating:

$$[M/H]_* = [O/H]_* = (12 + \log_{10}(O/H))_* - (12 + \log_{10}(O/H))_\odot \tag{4.1}$$

The solar oxygen abundance, $(12 + \log_{10}(O/H))_\odot = 8.69 \pm 0.05$ was sourced from Asplund et al. [5]. Redshifts, metallicities, and masses for this GRB host sample are presented in Table 4.1. These GRB hosts are plotted with several mass-metallicity relations in Figure 4.1. There is a ~ 0.6 dex shift toward lower metallicites in the MZ relation between z~ 0 to z~ 2. The GRB hosts clearly show a tendency toward lower metallicities, especially in lower mass galaxies. This GRB aversion to metallicity is expected at this redshift; as detailed in Chapter 3, GRB host galaxies are not expected to be unbiased tracers of star-formation until after $z \sim 3$. Furthermore the agreement of one GRB host with the Sanders et al. [76] $z \sim 2.3$ relation is notable, as the metallicity offset from the general MZ relation should be small at this redshift. This indicates that the methods used to create this figure were sound and that similar methods should be used to study our $z \sim 4.7$ sample.

In order to make a similar plot for the HST sample, masses and metallicities were collected from the literature. All literature-collected data for the HST sample of GRBs is presented in Table 4.4 at the end of this chapter. Many metallicities were offered as [S/H], but some were given as [Si/H] or as a blend of elements, [M/H]. These metallicities were converted to oxygen abundances as described above for the low-z sample. Masses were converted from magnitudes by first converting the observed-frame IR magnitudes provided by our collaborators (see Table 4.2) to rest-frame UV magnitudes via:

$$M_{UV} = m_{IR} - 5 * \log_{10}(d_L/10pc) + 2.5 * \log_{10}(1 + z) \tag{4.2}$$

GRB	Redshift	Metallicity ($12 + \log_{10}(O/H)$)	Metallicity (other)	$\log_{10}(M_*/M_\odot)$	Metallicity Ref.
050401	2.8983	7.69 ± 0.40	-1.0 ± 0.4 [Zn/H]	9.61	[92]
050820A	2.6147	7.09 ± 0.20	-1.5 ± 0.2 [Si/H]	9.38	[79]
050922C	2.1995	6.06 ± 0.05	-2.63 ± 0.01 [Fe/H]	< 9.01	[73]
080207	2.0858	8.74 ± 0.15	-	11.11	[52]
080210	2.6419	7.48 ± 0.17	-1.21 ± 0.16 [SiII/H]	< 9.50	[23]
080310	2.4274	7.3 ± 0.11	-1.39 ± 0.10 [O/H]	9.78	[27]

Table 4.1: Low Redshift Sample. Masses are from Perley et al. [71]. Metallicities were converted using Asplund et al. [5].

Here d_L is the “Luminosity Distance” and is calculated using a built-in *astropy* function using the redshift and assuming the cosmology from WMAP7 ($\Omega_m = 0.272$ and $H_0 = 70.4$ km/s/Mpc (Komatsu et al. [48])). The third term in equation (4.2) is the “K-correction” term; the k-correction addresses the fact that only part of the spectrum of the source is observed and is needed for non-local sources (Hogg et al. [39]). These absolute UV magnitudes were then converted to UV luminosities using the conversion from González et al. [32]:

$$M_{UV} = 51.63 - 2.5 * \log_{10}(L_{UV}) \tag{4.3}$$

Luminosities were then converted to masses using the conversion from González et al. [32]:

$$\log_{10}\left(\frac{M_*}{M_\odot}\right) = -39.6 + 1.7_{\pm 0.2} * \log_{10}(L_{UV}) \tag{4.4}$$

Uncertainties on the apparent magnitudes were provided by our collaborators. Uncertainties on the luminosities and masses were calculated as follows:

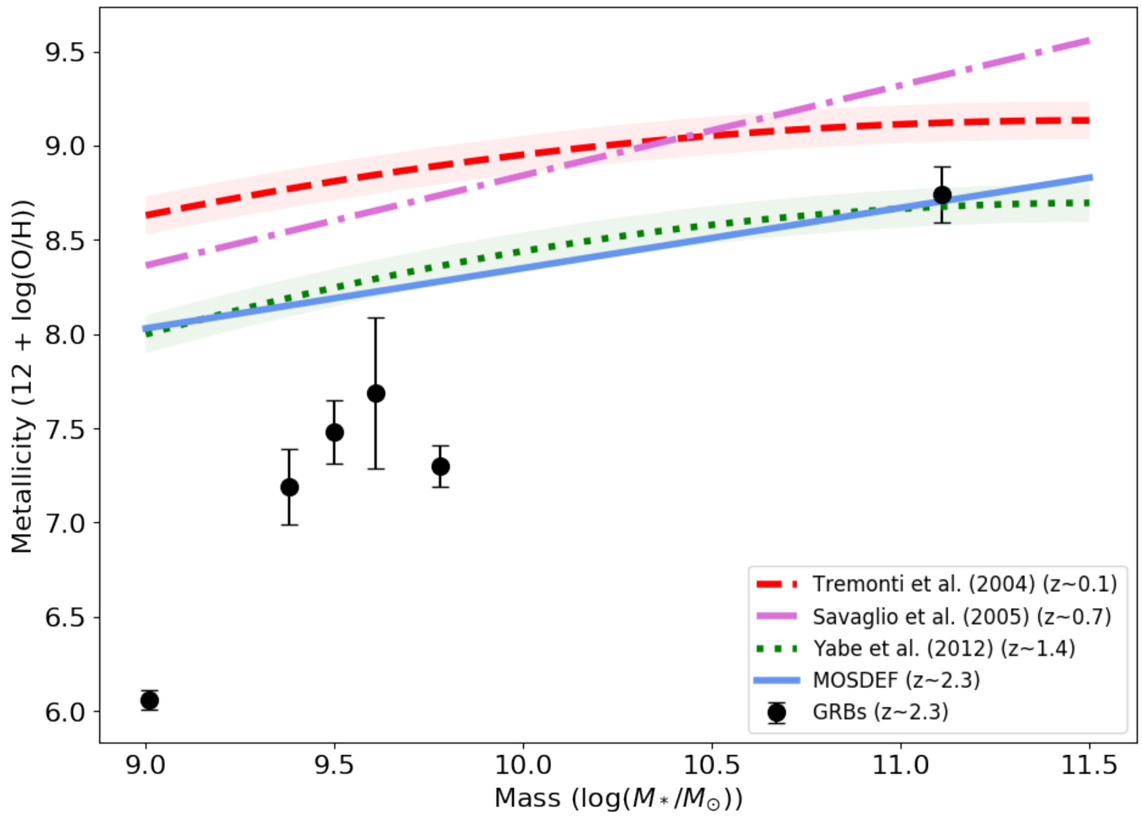

Figure 4.1: A mass-metallicity plot showing literature-collected GRBs at z~2.3 and mass-metallicity relations from Tremonti et al. [89], Savaglio et al. [78], Yabe et al. [95], and Sanders et al. [76]. A scatter of 0.1 dex was offered in both [89] and [95]. The relation from [76] was averaged from their three methods of metallicity determination. See Table 4.1 for GRB references.

$$L_{unc} = M_{UV,unc} * L * \ln(10)/-2.5 \tag{4.5}$$

$$\log_{10}\left(\frac{M_*}{M_\odot}\right)_{unc} = 1.7 * L_{unc}/L * \ln(10) \tag{4.6}$$

The uncertainty on the slope of equation (4.4) was ignored in calculating the uncertainty of the mass, as González et al. [32] states there is an intrinsic scatter of 0.5 dex in Eq. (4.4). The mass uncertainties displayed in Table 4.2 then just show the uncertainty propagated by the that of the luminosity. The masses and converted metallicites used to construct Figure 4.2 are presented in Table 4.3. When there was the option, published masses were selected over the magnitude-converted masses.

GRB	redshift	IR Magnitude	UV Magnitude	Mass ($\log_{10}(M_*/M_\odot)$)
120712A	4.175	26.27 ± 0.14	-19.88 ± 0.14	9.03 ± 0.19
140518A	4.7055	27.01 ± 0.19	-19.34 ± 0.19	8.66 ± 0.13
060510B	4.942	> 27.32	> -19.11	> 8.51
140311A	4.954	27.75 ± 0.42	-18.69 ± 0.42	8.22 ± 0.29
111008A	4.990	25.73 ± 0.08	-20.71 ± 0.08	9.60 ± 0.05

Table 4.2: HST Magnitudes. Observed-frame IR magnitudes were provided by our collaborators. These IR magnitudes were converted to rest-frame UV magnitudes and masses using [32]. Redshift references are in Table 4.4.

As mentioned above, at the end of this chapter Table 4.4 shows a collection of literature-reported values for the 23 GRBs in the HST sample. Metallicity and mass measurements were most immediately helpful for this project, though the neutral hydrogren column density and SFR will be used for later aspects of this project. The neutral hydrogen column density ($\log_{10}(N_{HI})$) has important relations back to the reionization of the early Universe; Chen et al. [15] has used the $\log_{10}(N_{HI})$ measured from GRB afterglows to trace the escape fraction of UV ionizing photons of star-forming galaxies. The star-formation rate (SFR) is highly dependent on the mass and metallicity of the host galaxy and a quantified M-Z-SFR rate has been found both in the local and far universe (Mannucci et al. [61], Lara-López et al. [56], Sanders et al. [76]).

Graham et al. [34] showed that, up to z$\sim$ 2.5, the distribution of GRB host galaxy metallicity and mass was redshift independent and found that the percentage of GRBs with high metallicity ($12 + \log_{10}(O/H) > 8.4$) was constant ($\sim 11\%$) with redshift. Several other publications have shown that GRBs are metal-averse above a metallicity threshold

GRB	Mass	Metallicity	Refs.
	$\log_{10}(M_*/M_\odot)$	$(12 + \log_{10}(O/H)_*)$	
060206	< 9.32	7.85 ± 0.11	[57],[28]
090516A	10.63	≥ 7.33	[86],[18]
120712A	< 9.82	< 8.31	[86],[10]
050505	< 9.67	≥ 7.49	[86],[7]
090205	< 10.7	> 8.12	[21]
100219A	< 10.11	7.53 ± 0.12	[86],[10]
140518A	8.66 ± 0.13	≥ 7.63	[18]
060510B	9.86	7.84 ± 0.16	[86],[14]
140311A	< 10.10	6.69 ± 0.12	[86],[10]
111008A	9.60 ± 0.05	6.99 ± 0.11	[82]
060927	< 9.48	≥ 7.14	[57],[18]

Table 4.3: Masses and Metallicities from the HST sample. Metallicites were converted using Asplund et al. (2009). Masses for GRB 140518A and 111008A were calculated from magnitudes, while all other masses were collected from literature.

(Perley et al. [71], Palmerio et al. [69]). Galaxies above redshift $z > 3$ should have metallicities below this threshold and so therefore GRBs should be unbiased tracers of star-formation after redshift $z > 3$ (Palmerio et al. [69], Greiner et al. [35]).

Surprisingly, the $z \sim 4$ sample of GRB hosts is still metal-poor when compared to $z \sim 3.5$ and $z \sim 8$ field galaxies, as shown in Figure 4.2. The average metallicity of the GRB sample is 7.54, which is $0.5 - 1$ dex offset below the $z \sim 2.3$ MZ relation from Sanders et al. [76] and, at maximum, 1 dex offset below the $z \sim 3.5$ relation from Maiolino et al. [60]. This offset is troubling as GRBs should be unbiased tracers at this redshift range and should therefore not have as large an offset, especially from the $z \sim 3.5$ relation.

That said, there appears to be continued evolution in the MZ relation of general star-forming galaxies past redshift $z \sim 3.5$, and it's notable that the average GRB metallicity is within the 0.5 dex uncertainty of the $z \sim 8$ relation from Jones et al. [43] throughout the plotted mass range. This is encouraging as it implies that at higher redshifts, GRBs are unbiased tracers of star-formation and that perhaps the metallicity threshold has not yet been broken in galaxies at $z \sim 3$.

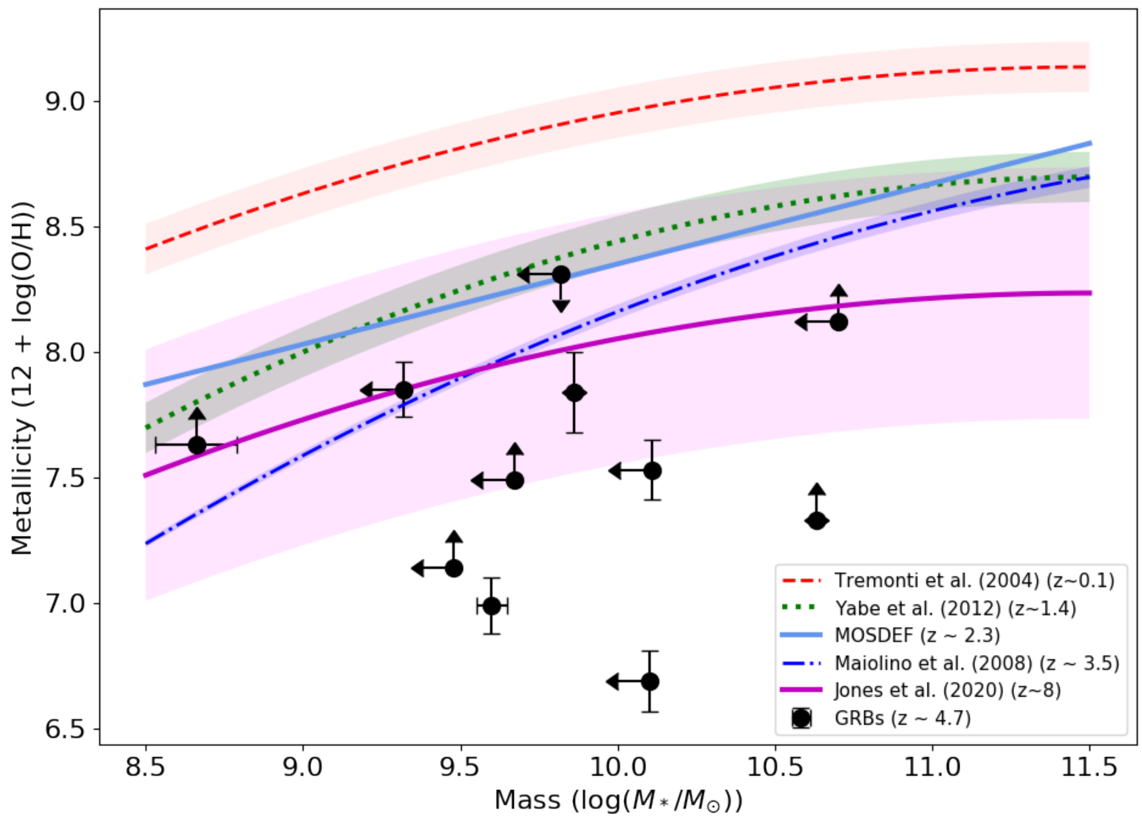

Figure 4.2: A mass-metallicity plot showing literature-collected GRBs at z~4.7 and mass-metallicity relations from Tremonti et al. [89], Yabe et al. [95], Sanders et al. [76], Maiolino et al. [60], and Jones et al. [43]. An uncertainty of 0.1 dex was offered in both [89] and [95]. The relation from [76] was averaged from their three methods of metallicity determination. Two MZ relations were offered in [60]; each were the best fit to data sets created with a different mass estimation method. The average of these two relations is shown in the dot-dashed line, while the uncertainty shading is the difference between the relations. Jones et al. [43] found that the $z \sim 8$ relation was just -0.9 ± 0.5 dex offset from the Tremonti et al. [89] relation. See Table 4.3 for GRB references.

4.3 Moving Forward

All but two of the masses used in Figure 4.2 were collected from the literature. Though our collaborators have only analyzed a few of the GRBs in the sample (displayed in Table 4.2 are their completed GRBs that also had published metallicities), once they are done, we will have magnitudes (and converted masses) for all 23 GRBs. 11 of these 23 GRBs have published metallicities, with an additional 7 having afterglow spectra that can be analyzed for possible metallicity measurements.

For the purposes of this project, observed-frame IR magnitudes were converted to luminosities. Using a mass-to-light ratio of z~ 4 galaxies (González et al. [32]), these luminosities were converted to masses. There are ways to more precisely convert a magnitude to a mass, and given the large uncertainty on the relationship (and lower limits of the literature-collected data), the plan is to use these methods for all of the GRBs in our sample. NASA's *Spitzer Space Telescope* images exist for all of the GRBs and probe the rest-frame optical (which is a more sensitive indicator of mass), but they are lacking in depth and are more susceptible to source confusion and contamination when compared to images taken with HST. The more resolved HST images will be essential in deconfusing the Spitzer images for accurate science. This is also why, when possible, published masses were chosen over our magnitude-converted masses for use in Figure 4.2.

While stellar mass estimates can be made from host galaxy imaging, metallicities for galaxies as faint as ours can only be directly determined from the afterglow spectra. Especially for galaxies at such high redshift, there is just no other source that is energetic enough to sufficiently illuminate the galaxy. Seven of the remaining 12 galaxies in this sample without published metallicities have afterglow spectra that can be analyzed further to obtain metallicity estimates. These estimates will be made by comparing various absorption line strengths as described in de Ugarte Postigo et al. [24]. In addition, it is important to be consistent when converting to gas-phase oxygen abundances. For the purposes of making Figure 4.2, it was assumed here that the oxygen to metal ratio was 1, i.e. $[O/H] = [M/H]$. Though this is an appropriate approximation, it is not exact, and care will need to be taken to find a more accurate ratio.

The plan moving forward is to establish whether GRB host galaxies follow the M-Z relationship of the star-forming galaxies and furthermore establish their association to the M-Z-SFR relation. In answering these questions, we will hopefully also determine if there is a M-Z relation for GRB host galaxies (as there has been at lower redshift (i.e. Levesque et al. [58])), and to quantify it, if so. Although the literature-collected data offers some guidance, ideally we will determine masses from the *Spitzer* images, constrain star-formation rates with HST images, and more accurately convert standard metallicities to gas-phase oxygen abundances.

Table 4.4: Properties of the $z \sim 4.7$ GRB Host Galaxy Sample

GRB	Redshift	Metallicity	Metallicity Type	$\log_{10}(N_{H1}/cm^{-2})$	SFR ($M_\odot/yr$)	$\log_{10}(M_*/M_\odot)$	Refs.
131117A	4.042	-	-	20.0 ± 0.3	-	-	[81]
060206	4.059	-0.84 ± 0.10	[S/H]	20.85 ± 0.10	1.2	< 9.32	[28],[35], [57]
090516A	4.109	≥ -1.36	[Si/H]	21.73 ± 0.10	20.4	10.63	[18], [24], [35], [86]
120712A	4.175	< -0.38	[S/H]	19.95 ± 0.15	-	< 9.82	[10], [81], [86]
140614A	4.233	-	-	21.6 ± 0.3	-	-	[81]
050505	4.275	≥ -1.2	[S/H]	22.05 ± 0.10	< 3.5	< 9.67	[7],[86]
050803	$4.3^{+0.4}_{-2.4}$	-	-	-	-	-	[71]
090205	4.6503	> -0.57	[S/H]	20.73 ± 0.05	4.2	< 10.7	[21]
100219A	4.667	-1.16 ± 0.11	[S/H]	21.20 ± 0.20	5.1	< 10.11	[81], [10],[35],[86]
140428A	$4.68^{+0.52}_{-0.18}$	-	-	-	-	-	[9]
140518A	4.7055	≥ -1.06	[S/H]	21.65 ± 0.20	-	-	[18]
100513A	4.772	-	-	21.80 ± 0.05	6.0	< 10.14	[86], [35]
071025	$4.8^{+0.4}_{-0.4}$	-	-	-	-	-	[71]
100302A	4.813	-	-	20.50 ± 0.30	-	-	[86]
050922B	4.9	-	-	-	-	-	[70]

GRB	Redshift	Metallicity	Metallicity Type	$\log_{10}(N_{H1}/cm^{-2})$	SFR $(M_\odot/yr)$	$\log_{10}(M_*/M_\odot)$	Refs.
060510B	4.942	-0.85 ± 0.15	[S/H]	21.3 ± 0.1	12.0	9.86	[14],[35],[86]
140311A	4.954	-2.00 ± 0.11	[M/H]	22.40 ± 0.15	-	< 10.10	[81],[10],[86]
111008A	4.990	-1.70 ± 0.10	[S/H]	22.30 ± 0.06	< 9.9	-	[82],[81],[35]
060522	5.110	-	-	21.0 ± 0.3	-	< 9.31	[14],[71]
050502B	$5.2^{+0.3}_{-0.3}$	-	-	-	-	-	[3]
140304A	5.283	-	-	21.6	-	-	[42]
060927	5.467	≥ -1.55	[S/H]	22.50 ± 0.15	< 0.65	< 9.48	[75],[18],[84],[57]
050814	$5.77^{0.12}_{0.12}$	-	-	-	-	9.93 ± 0.46	[57], [19]

5 Conclusion

It is important to know how our Galaxy came to be the way it is, and one such way to learn about our Galaxy's past is to study older galaxies. The evolution of chemical abundances in star-forming galaxies with redshift is an important indicator of several other galactic characteristics, such as the star-formation rate. The relation of a galaxy's chemical abundance (commonly referred to as its "metallicity") to its stellar mass is a common way to characterize this evolution.

Current methods to measure the metallicity of a galaxy can be difficult to use at high redshift. This is because at high redshift, galaxies are often too faint to allow for a sufficiently high signal-to-noise ratio spectrum for metallicities to be determined. As such, it is necessary to find other ways to measure a galaxy's metallicity. One such way is to use the spectrum from a GRB's afterglow. Before conclusions can be made from GRB afterglow spectroscopy, it must be established whether GRBs unbiasedly occur in general star-forming galaxies. At low redshift, it has been shown that GRBs preferentially occur in metal-poor star-forming galaxies and rarely burst in galaxies with a metallicity $12 + \log_{10}(O/H) >\sim 8.7$. Additionally it has been shown that there is not much time evolution of a GRB's metallicity preferences. Studies of the M-Z relation for general star-forming galaxies has shown there is evolution toward lower metallicities with increasing redshift, and it has been theorized that due to the evolution toward lower metallicities, after $z \sim 3$, GRBs should be unbiased tracers of star-formation. This would mean that GRB afterglow spectroscopy could be useful in studying the general properties of otherwise spectroscopically unobservable star-forming galaxies.

In order to first confirm that my methods would be useful at the redshift of our GRB host galaxy sample, I used them on a lesser redshift sample at $z \sim 2.3$. This redshift was chosen for comparison to the Sanders et al. [76] M-Z relation. It was shown in Figure 4.1 that, as expected, GRBs prefer more metal-poor hosts than general star-forming galaxies.

In studying the ~ 4.7 GRB host sample, it was first necessary to collect all literature-reported values for our galaxies. These are presented in Table 4.3. Most important for the study of the M-Z relation were, as expected, the mass and metallicity. As covered in Chapter 4, the neutral hydrogen column density and SFR will have use in further aspects of this project. Collaborators on this project measured observed-frame IR magnitudes for 7 GRB hosts in our sample. Using González et al. [32], I was able to convert these magnitudes to masses. Making assumptions about the metal distribution of the galaxies in our sample (namely that $\log_{10}(M/H)_* = \log_{10}(O/H)_*$) allowed me to convert all metallicities to gas-phase oxygen abundances. All galaxies in our sample that had both masses and metallicities to report were published in Figure 4.2. In comparing the trend of the GRB hosts to the published M-Z relations at various redshifts, it is evident that despite theoretical prediction, at $z \sim 4.7$, GRBs still prefer the most metal-poor star-forming galaxies. The agreement of our sample with the $z \sim 8$ relation is notable, though the large scatter on the relation necessitates more data and study.

Analysis of the remaining galaxies observed in the HST sample is ongoing. Future work will entail using *Spitzer* images to better constrain the mass of the GRB host galaxies and using more accurate metallicity conversions. Star-formation rates calculated from HST rest-frame UV magnitudes combined with the masses from the rest-frame optical *Spitzer* magnitudes will allow us to analyze the association of GRB hosts to the M-Z-SFR relation found at late times.

References

[1] K. N. Abazajian, J. K. Adelman-McCarthy, M. A. Agüeros, S. S. Allam, C. Allende Prieto, D. An, K. S. J. Anderson, S. F. Anderson, J. Annis, N. A. Bahcall, C. A. L. Bailer-Jones, J. C. Barentine, B. A. Bassett, A. C. Becker, T. C. Beers, E. F. Bell, V. Belokurov, A. A. Berlind, E. F. Berman, M. Bernardi, S. J. Bickerton, D. Bizyaev, J. P. Blakeslee, M. R. Blanton, J. J. Bochanski, W. N. Boroski, H. J. Brewington, J. Brinchmann, J. Brinkmann, R. J. Brunner, T. Budavári, L. N. Carey, S. Carliles, M. A. Carr, F. J. Castander, D. Cinabro, A. J. Connolly, I. Csabai, C. E. Cunha, P. C. Czarapata, J. R. A. Davenport, E. de Haas, B. Dilday, M. Doi, D. J. Eisenstein, M. L. Evans, N. W. Evans, X. Fan, S. D. Friedman, J. A. Frieman, M. Fukugita, B. T. Gänsicke, E. Gates, B. Gillespie, G. Gilmore, B. Gonzalez, C. F. Gonzalez, E. K. Grebel, J. E. Gunn, Z. Györy, P. B. Hall, P. Harding, F. H. Harris, M. Harvanek, S. L. Hawley, J. J. E. Hayes, T. M. Heckman, J. S. Hendry, G. S. Hennessy, R. B. Hindsley, J. Hoblitt, C. J. Hogan, D. W. Hogg, J. A. Holtzman, J. B. Hyde, S.-i. Ichikawa, T. Ichikawa, M. Im, Ž. Ivezić, S. Jester, L. Jiang, J. A. Johnson, A. M. Jorgensen, M. Jurić, S. M. Kent, R. Kessler, S. J. Kleinman, G. R. Knapp, K. Konishi, R. G. Kron, J. Krzesinski, N. Kuropatkin, H. Lampeitl, S. Lebedeva, M. G. Lee, Y. S. Lee, R. French Leger, S. Lépine, N. Li, M. Lima, H. Lin, D. C. Long, C. P. Loomis, J. Loveday, R. H. Lupton, E. Magnier, O. Malanushenko, V. Malanushenko, R. Mand elbaum, B. Margon, J. P. Marriner, D. Martínez-Delgado, T. Matsubara, P. M. McGehee, T. A. McKay, A. Meiksin, H. L. Morrison, F. Mullally, J. A. Munn, T. Murphy, T. Nash, A. Nebot, J. Neilsen, Eric H., H. J. Newberg, P. R. Newman, R. C. Nichol, T. Nicinski, M. Nieto-Santisteban, A. Nitta, S. Okamura, D. J. Oravetz, J. P. Ostriker, R. Owen, N. Padmanabhan, K. Pan, C. Park, G. Pauls, J. Peoples, John, W. J. Percival, J. R. Pier, A. C. Pope, D. Pourbaix, P. A. Price, N. Purger, T. Quinn, M. J. Raddick, P. Re Fiorentin, G. T. Richards, M. W. Richmond, A. G. Riess, H.-W. Rix, C. M. Rockosi, M. Sako, D. J. Schlegel, D. P. Schneider, R.-D. Scholz, M. R. Schreiber, A. D. Schwope, U. Seljak, B. Sesar, E. Sheldon, K. Shimasaku, V. C. Sibley, A. E. Simmons, T. Sivarani, J. Allyn Smith, M. C. Smith, V. Smolčić, S. A. Snedden, A. Stebbins, M. Steinmetz, C. Stoughton, M. A. Strauss, M. SubbaRao, Y. Suto, A. S. Szalay, I. Szapudi, P. Szkody, M. Tanaka, M. Tegmark, L. F. A. Teodoro, A. R. Thakar, C. A. Tremonti, D. L. Tucker, A. Uomoto, D. E. Vanden Berk, J. Vandenberg, S. Vidrih, M. S. Vogeley, W. Voges, N. P. Vogt, Y. Wadadekar, S. Watters, D. H. Weinberg, A. A. West, S. D. M. White, B. C. Wilhite, A. C. Wonders, B. Yanny, D. R. Yocum, D. G. York, I. Zehavi, S. Zibetti, and D. B. Zucker. The Seventh Data Release of the Sloan Digital Sky Survey. , 182(2): 543–558, June 2009. doi: 10.1088/0067-0049/182/2/543.

[2] B. P. Abbott et al. Gravitational waves and gamma-rays from a binary neutron star merger: GW170817 and GRB 170817a. *The Astrophysical Journal*, 848(2):L13, oct

2017. doi: 10.3847/2041-8213/aa920c. URL
https://doi.org/10.3847%2F2041-8213%2Faa920c.

[3] P. Afonso, J. Greiner, E. Pian, S. Covino, D. Malesani, A. Küpcü Yoldaș, T. Krühler, C. Clemens, S. McBreen, A. Rau, D. Giannios, and J. Hjorth. GRB 050502B optical afterglow: a jet-break at high redshift. , 526:A154, Feb. 2011. doi: 10.1051/0004-6361/200913965.

[4] B. H. Andrews and P. Martini. The Mass-Metallicity Relation with the Direct Method on Stacked Spectra of SDSS Galaxies. , 765(2):140, Mar. 2013. doi: 10.1088/0004-637X/765/2/140.

[5] M. Asplund, N. Grevesse, A. J. Sauval, and P. Scott. The Chemical Composition of the Sun. , 47(1):481–522, Sept. 2009. doi: 10.1146/annurev.astro.46.060407.145222.

[6] S. D. Barthelmy, L. M. Barbier, J. R. Cummings, E. E. Fenimore, N. Gehrels, D. Hullinger, H. A. Krimm, C. B. Markwardt, D. M. Palmer, A. Parsons, G. Sato, M. Suzuki, T. Takahashi, M. Tashiro, and J. Tueller. The Burst Alert Telescope (BAT) on the SWIFT Midex Mission. , 120(3-4):143–164, Oct. 2005. doi: 10.1007/s11214-005-5096-3.

[7] E. Berger, B. E. Penprase, S. B. Cenko, S. R. Kulkarni, D. B. Fox, C. C. Steidel, and N. A. Reddy. Spectroscopy of GRB 050505 at z = 4.275: A logN(H I) = 22.1 DLA Host Galaxy and the Nature of the Progenitor. , 642(2):979–988, May 2006. doi: 10.1086/501162.

[8] E. Berger, W. Fong, and R. Chornock. An r-process Kilonova Associated with the Short-hard GRB 130603B. , 774(2):L23, Sept. 2013. doi: 10.1088/2041-8205/774/2/L23.

[9] J. Bolmer, J. Greiner, T. Krühler, P. Schady, C. Ledoux, N. R. Tanvir, and A. J. Levan. Dust reddening and extinction curves toward gamma-ray bursts at z > 4. , 609:A62, Jan. 2018. doi: 10.1051/0004-6361/201731255.

[10] J. Bolmer, C. Ledoux, P. Wiseman, A. De Cia, J. Selsing, P. Schady, J. Greiner, S. Savaglio, J. M. Burgess, V. D'Elia, J. P. U. Fynbo, P. Goldoni, D. H. Hartmann, K. E. Heintz, P. Jakobsson, J. Japelj, L. Kaper, N. R. Tanvir, P. M. Vreeswijk, and T. Zafar. Evidence for diffuse molecular gas and dust in the hearts of gamma-ray burst host galaxies. Unveiling the nature of high-redshift damped Lyman-α systems. , 623:A43, Mar. 2019. doi: 10.1051/0004-6361/201834422.

[11] D. Branch and J. C. Wheeler. *Supernova explosions*. Springer-Verlag GmbH.

[12] J. Brinchmann, S. Charlot, S. D. M. White, C. Tremonti, G. Kauffmann, T. Heckman, and J. Brinkmann. The physical properties of star-forming galaxies in

the low-redshift Universe. , 351(4):1151–1179, July 2004. doi: 10.1111/j.1365-2966.2004.07881.x.

[13] S. Charlot and M. Longhetti. Nebular emission from star-forming galaxies. , 323(4): 887–903, May 2001. doi: 10.1046/j.1365-8711.2001.04260.x.

[14] R. Chary, E. Berger, and L. Cowie. Spitzer Observations of Gamma-Ray Burst Host Galaxies: A Unique Window into High-Redshift Chemical Evolution and Star Formation. , 671(1):272–277, Dec. 2007. doi: 10.1086/522692.

[15] H.-W. Chen, J. X. Prochaska, and N. Y. Gnedin. A New Constraint on the Escape Fraction in Distant Galaxies Using γ-Ray Burst Afterglow Spectroscopy. , 667(2): L125–L128, Oct. 2007. doi: 10.1086/522306.

[16] R. Chornock, E. Berger, D. B. Fox, R. Lunnan, M. R. Drout, W.-f. Fong, T. Laskar, and K. C. Roth. GRB 130606A as a Probe of the Intergalactic Medium and the Interstellar Medium in a Star-forming Galaxy in the First Gyr after the Big Bang. , 774(1):26, Sept. 2013. doi: 10.1088/0004-637X/774/1/26.

[17] A. A. Chrimes, E. R. Stanway, and J. J. Eldridge. Binary population synthesis models for core-collapse gamma-ray burst progenitors. , 491(3):3479–3495, Jan. 2020. doi: 10.1093/mnras/stz3246.

[18] A. Cucchiara, M. Fumagalli, M. Rafelski, D. Kocevski, J. X. Prochaska, R. J. Cooke, and G. D. Becker. Unveiling the Secrets of Metallicity and Massive Star Formation Using DLAs along Gamma-Ray Bursts. , 804(1):51, May 2015. doi: 10.1088/0004-637X/804/1/51.

[19] P. A. Curran, R. A. M. J. Wijers, M. H. M. Heemskerk, R. L. C. Starling, K. Wiersema, and A. J. van der Horst. Robust photometric redshift determinations of gamma-ray burst afterglows at z $\gtrsim$ 2. , 490(3):1047–1053, Nov. 2008. doi: 10.1051/0004-6361:200810545.

[20] M. Curti, F. Mannucci, G. Cresci, and R. Maiolino. The mass-metallicity and the fundamental metallicity relation revisited on a fully T_e-based abundance scale for galaxies. , 491(1):944–964, Jan. 2020. doi: 10.1093/mnras/stz2910.

[21] P. D'Avanzo, M. Perri, D. Fugazza, R. Salvaterra, G. Chincarini, R. Margutti, X. F. Wu, C. C. Thöne, A. Fernández-Soto, T. N. Ukwatta, D. N. Burrows, N. Gehrels, P. Meszaros, K. Toma, B. Zhang, S. Covino, S. Campana, V. D'Elia, M. Della Valle, and S. Piranomonte. The afterglow and host galaxy of GRB 090205: evidence of a Ly-α emitter at z = 4.65. , 522:A20, Nov. 2010. doi: 10.1051/0004-6361/201014801.

[22] M. Davis, S. M. Faber, J. Newman, A. C. Phillips, R. S. Ellis, C. C. Steidel, C. Conselice, A. L. Coil, D. P. Finkbeiner, D. C. Koo, P. Guhathakurta, B. Weiner,

R. Schiavon, C. Willmer, N. Kaiser, G. A. Luppino, G. Wirth, A. Connolly, P. Eisenhardt, M. Cooper, and B. Gerke. Science Objectives and Early Results of the DEEP2 Redshift Survey. In P. Guhathakurta, editor, *Discoveries and Research Prospects from 6- to 10-Meter-Class Telescopes II*, volume 4834 of *Society of Photo-Optical Instrumentation Engineers (SPIE) Conference Series*, pages 161–172, Feb. 2003. doi: 10.1117/12.457897.

[23] A. De Cia, P. Jakobsson, G. Björnsson, P. M. Vreeswijk, V. S. Dhillon, T. R. Marsh, R. Chapman, J. P. U. Fynbo, C. Ledoux, S. P. Littlefair, D. Malesani, S. Schulze, A. Smette, T. Zafar, and E. H. Gudmundsson. Probing gamma-ray burst environments with time variability: ULTRASPEC fast imaging of GRB 080210. , 412(4):2229–2240, Apr. 2011. doi: 10.1111/j.1365-2966.2010.18046.x.

[24] A. de Ugarte Postigo, J. P. U. Fynbo, C. C. Thöne, L. Christensen, J. Gorosabel, B. Milvang-Jensen, S. Schulze, P. Jakobsson, K. Wiersema, R. Sánchez-Ramírez, G. Leloudas, T. Zafar, D. Malesani, and J. Hjorth. The distribution of equivalent widths in long GRB afterglow spectra. , 548:A11, Dec. 2012. doi: 10.1051/0004-6361/201219894.

[25] J. P. Dezalay, C. Barat, R. Talon, R. Syunyaev, O. Terekhov, and A. Kuznetsov. Short Cosmic Events: A Subset of Classical GRBs? In W. S. Paciesas and G. J. Fishman, editors, *American Institute of Physics Conference Series*, volume 265 of *American Institute of Physics Conference Series*, page 304, Jan. 1992.

[26] D. K. Erb, A. E. Shapley, M. Pettini, C. C. Steidel, N. A. Reddy, and K. L. Adelberger. The Mass-Metallicity Relation at z>~2. , 644(2):813–828, June 2006. doi: 10.1086/503623.

[27] A. J. Fox, C. Ledoux, P. M. Vreeswijk, A. Smette, and A. O. Jaunsen. High-ion absorption in seven GRB host galaxies at z = 2-4. Evidence for both circumburst plasma and outflowing interstellar gas. , 491(1):189–207, Nov. 2008. doi: 10.1051/0004-6361:200810286.

[28] J. P. U. Fynbo, R. L. C. Starling, C. Ledoux, K. Wiersema, C. C. Thöne, J. Sollerman, P. Jakobsson, J. Hjorth, D. Watson, P. M. Vreeswijk, P. Møller, E. Rol, J. Gorosabel, J. Näränen, R. A. M. J. Wijers, G. Björnsson, J. M. Castro Cerón, P. Curran, D. H. Hartmann, S. T. Holland, B. L. Jensen, A. J. Levan, M. Limousin, C. Kouveliotou, G. Nelemans, K. Pedersen, R. S. Priddey, and N. R. Tanvir. Probing cosmic chemical evolution with gamma-ray bursts: GRB 060206 at z = 4.048. , 451 (3):L47–L50, June 2006. doi: 10.1051/0004-6361:20065056.

[29] T. J. Galama, P. M. Vreeswijk, J. van Paradijs, C. Kouveliotou, T. Augusteijn, H. Böhnhardt, J. P. Brewer, V. Doublier, J. F. Gonzalez, B. Leibundgut, C. Lidman, O. R. Hainaut, F. Patat, J. Heise, J. in't Zand, K. Hurley, P. J. Groot, R. G. Strom, P. A. Mazzali, K. Iwamoto, K. Nomoto, H. Umeda, T. Nakamura, T. R. Young,

T. Suzuki, T. Shigeyama, T. Koshut, M. Kippen, C. Robinson, P. de Wildt, R. A. M. J. Wijers, N. Tanvir, J. Greiner, E. Pian, E. Palazzi, F. Frontera, N. Masetti, L. Nicastro, M. Feroci, E. Costa, L. Piro, B. A. Peterson, C. Tinney, B. Boyle, R. Cannon, R. Stathakis, E. Sadler, M. C. Begam, and P. Ianna. An unusual supernova in the error box of the γ-ray burst of 25 April 1998. , 395(6703):670–672, Oct. 1998. doi: 10.1038/27150.

[30] N. Gehrels, E. Ramirez-Ruiz, and D. B. Fox. Gamma-Ray Bursts in the Swift Era. , 47(1):567–617, Sept. 2009. doi: 10.1146/annurev.astro.46.060407.145147.

[31] M. J. Geller, I. P. Dell'Antonio, M. J. Kurtz, M. Ramella, D. G. Fabricant, N. Caldwell, J. A. Tyson, and D. Wittman. SHELS: The Hectospec Lensing Survey. , 635(2):L125–L128, Dec. 2005. doi: 10.1086/499399.

[32] V. González, I. Labbé, R. J. Bouwens, G. Illingworth, M. Franx, and M. Kriek. Evolution of Galaxy Stellar Mass Functions, Mass Densities, and Mass-to-light Ratios from z ~7 to z ~4. , 735(2):L34, July 2011. doi: 10.1088/2041-8205/735/2/L34.

[33] J. F. Graham and A. S. Fruchter. The Metal Aversion of Long-duration Gamma-Ray Bursts. , 774(2):119, Sept. 2013. doi: 10.1088/0004-637X/774/2/119.

[34] J. F. Graham, P. Schady, and A. S. Fruchter. A Surprising Lack of LGRB Metallicity Evolution with Redshift. *arXiv e-prints*, art. arXiv:1904.02673, Apr. 2019.

[35] J. Greiner, D. B. Fox, P. Schady, T. Krühler, M. Trenti, A. Cikota, J. Bolmer, J. Elliott, C. Delvaux, R. Perna, P. Afonso, D. A. Kann, S. Klose, S. Savaglio, S. Schmidl, T. Schweyer, M. Tanga, and K. Varela. Gamma-Ray Bursts Trace UV Metrics of Star Formation over 3 < z < 5. , 809(1):76, Aug. 2015. doi: 10.1088/0004-637X/809/1/76.

[36] J. Greiner, P. A. Mazzali, D. A. Kann, T. Krühler, E. Pian, S. Prentice, F. Olivares E., A. Rossi, S. Klose, S. Taubenberger, F. Knust, P. M. J. Afonso, C. Ashall, J. Bolmer, C. Delvaux, R. Diehl, J. Elliott, R. Filgas, J. P. U. Fynbo, J. F. Graham, A. N. Guelbenzu, S. Kobayashi, G. Leloudas, S. Savaglio, P. Schady, S. Schmidl, T. Schweyer, V. Sudilovsky, M. Tanga, A. C. Updike, H. van Eerten, and K. Varela. A very luminous magnetar-powered supernova associated with an ultra-long γ-ray burst. , 523(7559):189–192, July 2015. doi: 10.1038/nature14579.

[37] X. H. Han, F. Hammer, Y. C. Liang, H. Flores, M. Rodrigues, J. L. Hou, and J. Y. Wei. The Wolf-Rayet features and mass-metallicity relation of long-duration gamma-ray burst host galaxies. , 514:A24, May 2010. doi: 10.1051/0004-6361/200912475.

[38] J. Hjorth and J. S. Bloom. *The Gamma-Ray Burst - Supernova Connection*, pages 169–190. 2012.

[39] D. W. Hogg, I. K. Baldry, M. R. Blanton, and D. J. Eisenstein. The K correction. *arXiv e-prints*, art. astro-ph/0210394, Oct. 2002.

[40] J. D. Hunter. Matplotlib: A 2d graphics environment. *Computing in Science & Engineering*, 9(3):90–95, 2007. doi: 10.1109/MCSE.2007.55.

[41] J. Japelj, S. D. Vergani, R. Salvaterra, M. Renzo, E. Zapartas, S. E. de Mink, L. Kaper, and S. Zibetti. Host galaxies of SNe Ic-BL with and without long gamma-ray bursts. , 617:A105, Sept. 2018. doi: 10.1051/0004-6361/201833209.

[42] S. Jeong, R. Sanchez-Ramirez, J. Gorosabel, and A. J. Castro-Tirado. GRB 140304A: 10.4m GTC refined redshift z = 5.283. *GRB Coordinates Network*, 15936: 1, Jan. 2014.

[43] T. Jones, R. Sanders, G. Roberts-Borsani, R. S. Ellis, N. Laporte, T. Treu, and Y. Harikane. The Mass-Metallicity Relation at z=8: Direct-Method Metallicity Constraints and Near-Future Prospects. *arXiv e-prints*, art. arXiv:2006.02447, June 2020.

[44] G. Kauffmann, T. M. Heckman, S. D. M. White, S. Charlot, C. Tremonti, J. Brinchmann, G. Bruzual, E. W. Peng, M. Seibert, M. Bernardi, M. Blanton, J. Brinkmann, F. Castander, I. Csábai, M. Fukugita, Z. Ivezic, J. A. Munn, R. C. Nichol, N. Padmanabhan, A. R. Thakar, D. H. Weinberg, and D. York. Stellar masses and star formation histories for 10^5 galaxies from the Sloan Digital Sky Survey. , 341(1):33–53, May 2003. doi: 10.1046/j.1365-8711.2003.06291.x.

[45] G. Kauffmann, S. D. M. White, T. M. Heckman, B. Ménard, J. Brinchmann, S. Charlot, C. Tremonti, and J. Brinkmann. The environmental dependence of the relations between stellar mass, structure, star formation and nuclear activity in galaxies. , 353(3):713–731, Sept. 2004. doi: 10.1111/j.1365-2966.2004.08117.x.

[46] R. W. Klebesadel, I. B. Strong, and R. A. Olson. Observations of Gamma-Ray Bursts of Cosmic Origin. , 182:L85, June 1973. doi: 10.1086/181225.

[47] T. Kluyver, B. Ragan-Kelley, F. Pérez, B. Granger, M. Bussonnier, J. Frederic, K. Kelley, J. Hamrick, J. Grout, S. Corlay, P. Ivanov, D. Avila, S. Abdalla, and C. Willing. Jupyter notebooks – a publishing format for reproducible computational workflows. In F. Loizides and B. Schmidt, editors, *Positioning and Power in Academic Publishing: Players, Agents and Agendas*, pages 87 – 90. IOS Press, 2016.

[48] E. Komatsu, K. M. Smith, J. Dunkley, C. L. Bennett, B. Gold, G. Hinshaw, N. Jarosik, D. Larson, M. R. Nolta, L. Page, D. N. Spergel, M. Halpern, R. S. Hill, A. Kogut, M. Limon, S. S. Meyer, N. Odegard, G. S. Tucker, J. L. Weiland, E. Wollack, and E. L. Wright. Seven-year Wilkinson Microwave Anisotropy Probe (WMAP) Observations: Cosmological Interpretation. , 192(2):18, Feb. 2011. doi: 10.1088/0067-0049/192/2/18.

[49] C. Kouveliotou, C. A. Meegan, G. J. Fishman, N. P. Bhat, M. S. Briggs, T. M. Koshut, W. S. Paciesas, and G. N. Pendleton. Identification of Two Classes of Gamma-Ray Bursts. , 413:L101, Aug. 1993. doi: 10.1086/186969.

[50] C. Kouveliotou, S. E. Woosley, S. K. Patel, A. Levan, R. Blandford, E. Ramirez-Ruiz, R. A. M. J. Wijers, M. C. Weisskopf, A. Tennant, E. Pian, and P. Giommi. Chandra Observations of the X-Ray Environs of SN 1998bw/GRB 980425. , 608(2):872–882, June 2004. doi: 10.1086/420878.

[51] M. Kriek, A. E. Shapley, N. A. Reddy, B. Siana, A. L. Coil, B. Mobasher, W. R. Freeman, L. de Groot, S. H. Price, R. Sanders, I. Shivaei, G. B. Brammer, I. G. Momcheva, R. E. Skelton, P. G. van Dokkum, K. E. Whitaker, J. Aird, M. Azadi, M. Kassis, J. S. Bullock, C. Conroy, R. Davé, D. Kereš, and M. Krumholz. The MOSFIRE Deep Evolution Field (MOSDEF) Survey: Rest-frame Optical Spectroscopy for ~1500 H-selected Galaxies at 1.37 ¡ z ¡ 3.8. , 218(2):15, June 2015. doi: 10.1088/0067-0049/218/2/15.

[52] T. Krühler, D. Malesani, J. P. U. Fynbo, O. E. Hartoog, J. Hjorth, P. Jakobsson, D. A. Perley, A. Rossi, P. Schady, S. Schulze, N. R. Tanvir, S. D. Vergani, K. Wiersema, P. M. J. Afonso, J. Bolmer, Z. Cano, S. Covino, V. D'Elia, A. de Ugarte Postigo, R. Filgas, M. Friis, J. F. Graham, J. Greiner, P. Goldoni, A. Gomboc, F. Hammer, J. Japelj, D. A. Kann, L. Kaper, S. Klose, A. J. Levan, G. Leloudas, B. Milvang-Jensen, A. Nicuesa Guelbenzu, E. Palazzi, E. Pian, S. Piranomonte, R. Sánchez-Ramírez, S. Savaglio, J. Selsing, G. Tagliaferri, P. M. Vreeswijk, D. J. Watson, and D. Xu. GRB hosts through cosmic time. VLT/X-Shooter emission-line spectroscopy of 96 γ-ray-burst-selected galaxies at 0.1 <z < 3.6. , 581:A125, Sept. 2015. doi: 10.1051/0004-6361/201425561.

[53] C. Laigle, H. J. McCracken, O. Ilbert, B. C. Hsieh, I. Davidzon, P. Capak, G. Hasinger, J. D. Silverman, C. Pichon, J. Coupon, H. Aussel, D. Le Borgne, K. Caputi, P. Cassata, Y. Y. Chang, F. Civano, J. Dunlop, J. Fynbo, J. S. Kartaltepe, A. Koekemoer, O. Le Fèvre, E. Le Floc'h, A. Leauthaud, S. Lilly, L. Lin, S. Marchesi, B. Milvang-Jensen, M. Salvato, D. B. Sanders, N. Scoville, V. Smolcic, M. Stockmann, Y. Taniguchi, L. Tasca, S. Toft, M. Vaccari, and J. Zabl. The COSMOS2015 Catalog: Exploring the 1 ¡ z ¡ 6 Universe with Half a Million Galaxies. , 224(2):24, June 2016. doi: 10.3847/0067-0049/224/2/24.

[54] M. A. Lara-López, J. Cepa, A. Bongiovanni, H. Castañeda, A. M. Pérez García, M. Fernández Lorenzo, M. Póvic, and M. Sánchez-Portal. Star-forming galaxies in SDSS: signs of metallicity evolution. , 493(1):L5–L8, Jan. 2009. doi: 10.1051/0004-6361:200811033.

[55] M. A. Lara-López, J. Cepa, A. Bongiovanni, A. M. Pérez García, H. Castañeda, M. Fernández Lorenzo, M. Pović, and M. Sánchez-Portal. Study of star-forming

galaxies in SDSS up to redshift 0.4. I. Metallicity evolution. , 505(2):529–539, Oct. 2009. doi: 10.1051/0004-6361/200912214.

[56] M. A. Lara-López, J. Cepa, A. Bongiovanni, A. M. Pérez García, A. Ederoclite, H. Castañeda, M. Fernández Lorenzo, M. Pović, and M. Sánchez-Portal. A fundamental plane for field star-forming galaxies. , 521:L53, Oct. 2010. doi: 10.1051/0004-6361/201014803.

[57] T. Laskar, E. Berger, and R.-R. Chary. Exploring the Galaxy Mass-metallicity Relation at z ~3-5. , 739(1):1, Sept. 2011. doi: 10.1088/0004-637X/739/1/1.

[58] E. M. Levesque, L. J. Kewley, E. Berger, and H. J. Zahid. The Host Galaxies of Gamma-ray Bursts. II. A Mass-metallicity Relation for Long-duration Gamma-ray Burst Host Galaxies. , 140(5):1557–1566, Nov. 2010. doi: 10.1088/0004-6256/140/5/1557.

[59] A. I. MacFadyen and S. E. Woosley. Collapsars: Gamma-Ray Bursts and Explosions in “Failed Supernovae”. , 524(1):262–289, Oct. 1999. doi: 10.1086/307790.

[60] R. Maiolino, T. Nagao, A. Grazian, F. Cocchia, A. Marconi, F. Mannucci, A. Cimatti, A. Pipino, S. Ballero, F. Calura, C. Chiappini, A. Fontana, G. L. Granato, F. Matteucci, G. Pastorini, L. Pentericci, G. Risaliti, M. Salvati, and L. Silva. AMAZE. I. The evolution of the mass-metallicity relation at z > 3. , 488(2): 463–479, Sept. 2008. doi: 10.1051/0004-6361:200809678.

[61] F. Mannucci, G. Cresci, R. Maiolino, A. Marconi, and A. Gnerucci. A fundamental relation between mass, star formation rate and metallicity in local and high-redshift galaxies. , 408(4):2115–2127, Nov. 2010. doi: 10.1111/j.1365-2966.2010.17291.x.

[62] F. Mannucci, R. Salvaterra, and M. A. Campisi. The metallicity of the long GRB hosts and the fundamental metallicity relation of low-mass galaxies. , 414(2): 1263–1268, June 2011. doi: 10.1111/j.1365-2966.2011.18459.x.

[63] T. Matheson, P. M. Garnavich, K. Z. Stanek, D. Bersier, S. T. Holland, K. Krisciunas, N. Caldwell, P. Berlind, J. S. Bloom, M. Bolte, A. Z. Bonanos, M. J. I. Brown, W. R. Brown, M. L. Calkins, P. Challis, R. Chornock, L. Echevarria, D. J. Eisenstein, M. E. Everett, A. V. Filippenko, K. Flint, R. J. Foley, D. L. Freedman, M. Hamuy, P. Harding, N. P. Hathi, M. Hicken, C. Hoopes, C. Impey, B. T. Jannuzi, R. A. Jansen, S. Jha, J. Kaluzny, S. Kannappan, R. P. Kirshner, D. W. Latham, J. C. Lee, D. C. Leonard, W. Li, K. L. Luhman, P. Martini, H. Mathis, J. Maza, S. T. Megeath, L. R. Miller, D. Minniti, E. W. Olszewski, M. Papenkova, M. M. Phillips, B. Pindor, D. D. Sasselov, R. Schild, H. Schweiker, T. Spahr, J. Thomas-Osip, I. Thompson, D. Weisz, R. Windhorst, and D. Zaritsky. Photometry and Spectroscopy of GRB 030329 and Its Associated Supernova 2003dh: The First Two Months. , 599(1):394–407, Dec. 2003. doi: 10.1086/379228.

[64] J. T. W. McGuire, N. R. Tanvir, A. J. Levan, M. Trenti, E. R. Stanway, J. M. Shull, K. Wiersema, D. A. Perley, R. L. C. Starling, M. Bremer, J. T. Stocke, J. Hjorth, J. E. Rhoads, E. Curtis-Lake, S. Schulze, E. M. Levesque, B. Robertson, J. P. U. Fynbo, R. S. Ellis, and A. S. Fruchter. Detection of Three Gamma-ray Burst Host Galaxies at z 6. , 825(2):135, July 2016. doi: 10.3847/0004-637X/825/2/135.

[65] A. McWilliam. Abundance Ratios and Galactic Chemical Evolution. , 35:503–556, Jan. 1997. doi: 10.1146/annurev.astro.35.1.503.

[66] B. Metha and M. Trenti. One star, two stars, or both? Investigating metallicity-dependent models for gamma-ray burst progenitors with the IllustrisTNG simulation. , 495(1):266–277, Apr. 2020. doi: 10.1093/mnras/staa1114.

[67] E. Nakar. Short-hard gamma-ray bursts. , 442(1-6):166–236, Apr. 2007. doi: 10.1016/j.physrep.2007.02.005.

[68] T. E. Oliphant. *A guide to NumPy*, volume 1. Trelgol Publishing USA, 2006.

[69] J. T. Palmerio, S. D. Vergani, R. Salvaterra, R. L. Sand ers, J. Japelj, A. Vidal-García, P. D'Avanzo, D. Corre, D. A. Perley, A. E. Shapley, S. Boissier, J. Greiner, E. Le Floc'h, and P. Wiseman. Are long gamma-ray bursts biased tracers of star formation? Clues from the host galaxies of the Swift/BAT6 complete sample of bright LGRBs. III. Stellar masses, star formation rates, and metallicities at z > 1. , 623:A26, Mar. 2019. doi: 10.1051/0004-6361/201834179.

[70] D. A. Perley, T. Krühler, S. Schulze, A. de Ugarte Postigo, J. Hjorth, E. Berger, S. B. Cenko, R. Chary, A. Cucchiara, R. Ellis, W. Fong, J. P. U. Fynbo, J. Gorosabel, J. Greiner, P. Jakobsson, S. Kim, T. Laskar, A. J. Levan, M. J. Michałowski, B. Milvang-Jensen, N. R. Tanvir, C. C. Thöne, and K. Wiersema. The Swift Gamma-Ray Burst Host Galaxy Legacy Survey. I. Sample Selection and Redshift Distribution. , 817(1):7, Jan. 2016. doi: 10.3847/0004-637X/817/1/7.

[71] D. A. Perley, N. R. Tanvir, J. Hjorth, T. Laskar, E. Berger, R. Chary, A. de Ugarte Postigo, J. P. U. Fynbo, T. Krühler, A. J. Levan, M. J. Michałowski, and S. Schulze. The Swift GRB Host Galaxy Legacy Survey. II. Rest-frame Near-IR Luminosity Distribution and Evidence for a Near-solar Metallicity Threshold. , 817(1):8, Jan. 2016. doi: 10.3847/0004-637X/817/1/8.

[72] R. D. Preece, M. S. Briggs, R. S. Mallozzi, G. N. Pendleton, W. S. Paciesas, and D. L. Band. The BATSE Gamma-Ray Burst Spectral Catalog. I. High Time Resolution Spectroscopy of Bright Bursts Using High Energy Resolution Data. , 126 (1):19–36, Jan. 2000. doi: 10.1086/313289.

[73] J. X. Prochaska, H.-W. Chen, M. Dessauges-Zavadsky, and J. S. Bloom. Probing the Interstellar Medium near Star-forming Regions with Gamma-Ray Burst Afterglow

Spectroscopy: Gas, Metals, and Dust. , 666(1):267–280, Sept. 2007. doi: 10.1086/520042.

[74] M. Rodrigues, F. Hammer, H. Flores, M. Puech, Y. C. Liang, I. Fuentes-Carrera, N. Nesvadba, M. Lehnert, Y. Yang, P. Amram, C. Balkowski, C. Cesarsky, H. Dannerbauer, R. Delgado, B. Guiderdoni, A. Kembhavi, B. Neichel, G. Östlin, L. Pozzetti, C. D. Ravikumar, A. Rawat, S. di Serego Alighieri, D. Vergani, J. Vernet, and H. Wozniak. IMAGES IV: strong evolution of the oxygen abundance in gaseous phases of intermediate mass galaxies from z ~0.8. , 492(2):371–388, Dec. 2008. doi: 10.1051/0004-6361:200810435.

[75] A. E. Ruiz-Velasco, H. Swan, E. Troja, D. Malesani, J. P. U. Fynbo, R. L. C. Starling, D. Xu, F. Aharonian, C. Akerlof, M. I. Andersen, M. C. B. Ashley, S. D. Barthelmy, D. Bersier, J. M. Castro Cerón, A. J. Castro-Tirado, N. Gehrels, E. Göğüş, J. Gorosabel, C. Guidorzi, T. Güver, J. Hjorth, D. Horns, K. Y. Huang, P. Jakobsson, B. L. Jensen, Ü. Kızıloğlu, C. Kouveliotou, H. A. Krimm, C. Ledoux, A. J. Levan, T. Marsh, T. McKay, A. Melandri, B. Milvang-Jensen, C. G. Mundell, P. T. O'Brien, M. Özel, A. Phillips, R. Quimby, G. Rowell, W. Rujopakarn, E. S. Rykoff, B. E. Schaefer, J. Sollerman, N. R. Tanvir, C. C. Thöne, Y. Urata, W. T. Vestrand , P. M. Vreeswijk, D. Watson, J. C. Wheeler, R. A. M. J. Wijers, J. Wren, S. A. Yost, F. Yuan, M. Zhai, and W. K. Zheng. Detection of GRB 060927 at z = 5.47: Implications for the Use of Gamma-Ray Bursts as Probes of the End of the Dark Ages. , 669(1):1–9, Nov. 2007. doi: 10.1086/521546.

[76] R. L. Sanders, A. E. Shapley, M. Kriek, W. R. Freeman, N. A. Reddy, B. Siana, A. L. Coil, B. Mobasher, R. Davé, I. Shivaei, M. Azadi, S. H. Price, G. Leung, T. Fetherolf, L. de Groot, T. Zick, F. M. Fornasini, and G. Barro. The MOSDEF Survey: A Stellar Mass-SFR-Metallicity Relation Exists at z 2.3. , 858(2):99, May 2018. doi: 10.3847/1538-4357/aabcbd.

[77] R. L. Sanders, A. E. Shapley, N. A. Reddy, M. Kriek, B. Siana, A. L. Coil, B. Mobasher, I. Shivaei, W. R. Freeman, M. Azadi, S. H. Price, G. Leung, T. Fetherolf, L. de Groot, T. Zick, F. M. Fornasini, and G. Barro. The MOSDEF survey: direct-method metallicities and ISM conditions at z $\sim$ 1.5-3.5. , 491(1): 1427–1455, Jan. 2020. doi: 10.1093/mnras/stz3032.

[78] S. Savaglio, K. Glazebrook, D. Le Borgne, S. Juneau, R. G. Abraham, H. W. Chen, D. Crampton, P. J. McCarthy, R. G. Carlberg, R. O. Marzke, K. Roth, I. Jørgensen, and R. Murowinski. The Gemini Deep Deep Survey. VII. The Redshift Evolution of the Mass-Metallicity Relation. , 635(1):260–279, Dec. 2005. doi: 10.1086/497331.

[79] S. Schulze, J. P. U. Fynbo, B. Milvang-Jensen, A. Rossi, P. Jakobsson, C. Ledoux, A. De Cia, T. Krühler, A. Mehner, G. Björnsson, H. W. Chen, P. M. Vreeswijk, D. A. Perley, J. Hjorth, A. J. Levan, N. R. Tanvir, S. Ellison, P. Møller, G. Worseck, R. Chapman, A. Dall'Aglio, and G. Letawe. Galaxy counterparts of intervening

high-z sub-DLAs/DLAs and Mg ii absorbers towards gamma-ray bursts. , 546:A20, Oct. 2012. doi: 10.1051/0004-6361/201118647.

[80] S. Schulze, D. Malesani, A. Cucchiara, N. R. Tanvir, T. Krühler, A. de Ugarte Postigo, G. Leloudas, J. Lyman, D. Bersier, K. Wiersema, D. A. Perley, P. Schady, J. Gorosabel, J. P. Anderson, A. J. Castro-Tirado, S. B. Cenko, A. De Cia, L. E. Ellerbroek, J. P. U. Fynbo, J. Greiner, J. Hjorth, D. A. Kann, L. Kaper, S. Klose, A. J. Levan, S. Martín, P. T. O'Brien, K. L. Page, G. Pignata, S. Rapaport, R. Sánchez-Ramírez, J. Sollerman, I. A. Smith, M. Sparre, C. C. Thöne, D. J. Watson, D. Xu, F. E. Bauer, M. Bayliss, G. Björnsson, M. Bremer, Z. Cano, S. Covino, V. D'Elia, D. A. Frail, S. Geier, P. Goldoni, O. E. Hartoog, P. Jakobsson, H. Korhonen, K. Y. Lee, B. Milvang-Jensen, M. Nardini, A. Nicuesa Guelbenzu, M. Oguri, S. B. Pandey, G. Petitpas, A. Rossi, A. Sandberg, S. Schmidl, G. Tagliaferri, R. P. J. Tilanus, J. M. Winters, D. Wright, and E. Wuyts. GRB 120422A/SN 2012bz: Bridging the gap between low- and high-luminosity gamma-ray bursts. , 566:A102, June 2014. doi: 10.1051/0004-6361/201423387.

[81] J. Selsing, D. Malesani, P. Goldoni, J. P. U. Fynbo, T. Krühler, L. A. Antonelli, M. Arabsalmani, J. Bolmer, Z. Cano, L. Christensen, S. Covino, P. D'Avanzo, V. D'Elia, A. De Cia, A. de Ugarte Postigo, H. Flores, M. Friis, A. Gomboc, J. Greiner, P. Groot, F. Hammer, O. E. Hartoog, K. E. Heintz, J. Hjorth, P. Jakobsson, J. Japelj, D. A. Kann, L. Kaper, C. Ledoux, G. Leloudas, A. J. Levan, E. Maiorano, A. Melandri, B. Milvang-Jensen, E. Palazzi, J. T. Palmerio, D. A. Perley, E. Pian, S. Piranomonte, G. Pugliese, R. Sánchez-Ramírez, S. Savaglio, P. Schady, S. Schulze, J. Sollerman, M. Sparre, G. Tagliaferri, N. R. Tanvir, C. C. Thöne, S. D. Vergani, P. Vreeswijk, D. Watson, K. Wiersema, R. Wijers, D. Xu, and T. Zafar. The X-shooter GRB afterglow legacy sample (XS-GRB). , 623:A92, Mar. 2019. doi: 10.1051/0004-6361/201832835.

[82] M. Sparre, O. E. Hartoog, T. Krühler, J. P. U. Fynbo, D. J. Watson, K. Wiersema, V. D'Elia, T. Zafar, P. M. J. Afonso, S. Covino, A. de Ugarte Postigo, H. Flores, P. Goldoni, J. Greiner, J. Hjorth, P. Jakobsson, L. Kaper, S. Klose, A. J. Levan, D. Malesani, B. Milvang-Jensen, M. Nardini, S. Piranomonte, J. Sollerman, R. Sánchez-Ramírez, S. Schulze, N. R. Tanvir, S. D. Vergani, and R. A. M. J. Wijers. The Metallicity and Dust Content of a Redshift 5 Gamma-Ray Burst Host Galaxy. , 785(2):150, Apr. 2014. doi: 10.1088/0004-637X/785/2/150.

[83] K. Z. Stanek, O. Y. Gnedin, J. F. Beacom, A. P. Gould, J. A. Johnson, J. A. Kollmeier, M. Modjaz, M. H. Pinsonneault, R. Pogge, and D. H. Weinberg. Protecting Life in the Milky Way: Metals Keep the GRBs Away. , 56:333–345, Dec. 2006.

[84] N. R. Tanvir, A. J. Levan, A. S. Fruchter, J. P. U. Fynbo, J. Hjorth, K. Wiersema, M. N. Bremer, J. Rhoads, P. Jakobsson, P. T. O'Brien, E. R. Stanway, D. Bersier,

P. Natarajan, J. Greiner, D. Watson, A. J. Castro-Tirado, R. A. M. J. Wijers, R. L. C. Starling, K. Misra, J. F. Graham, and C. Kouveliotou. Star Formation in the Early Universe: Beyond the Tip of the Iceberg. , 754(1):46, July 2012. doi: 10.1088/0004-637X/754/1/46.

[85] N. R. Tanvir, A. J. Levan, A. S. Fruchter, J. Hjorth, R. A. Hounsell, K. Wiersema, and R. L. Tunnicliffe. A ‘kilonova’ associated with the short-duration γ-ray burst GRB 130603B. , 500(7464):547–549, Aug. 2013. doi: 10.1038/nature12505.

[86] N. R. Tanvir, J. P. U. Fynbo, A. de Ugarte Postigo, J. Japelj, K. Wiersema, D. Malesani, D. A. Perley, A. J. Levan, J. Selsing, S. B. Cenko, D. A. Kann, B. Milvang-Jensen, E. Berger, Z. Cano, R. Chornock, S. Covino, A. Cucchiara, V. D’Elia, A. Gargiulo, P. Goldoni, A. Gomboc, K. E. Heintz, J. Hjorth, L. Izzo, P. Jakobsson, L. Kaper, T. Krühler, T. Laskar, M. Myers, S. Piranomonte, G. Pugliese, A. Rossi, R. Sánchez-Ramírez, S. Schulze, M. Sparre, E. R. Stanway, G. Tagliaferri, C. C. Thöne, S. Vergani, P. M. Vreeswijk, R. A. M. J. Wijers, D. Watson, and D. Xu. The fraction of ionizing radiation from massive stars that escapes to the intergalactic medium. , 483(4):5380–5408, Mar. 2019. doi: 10.1093/mnras/sty3460.

[87] B. M. Tinsley. Stellar lifetimes and abundance ratios in chemical evolution. , 229: 1046–1056, May 1979. doi: 10.1086/157039.

[88] V. L. Toy, S. B. Cenko, J. M. Silverman, N. R. Butler, A. Cucchiara, A. M. Watson, D. Bersier, D. A. Perley, R. Margutti, E. Bellm, J. S. Bloom, Y. Cao, J. I. Capone, K. Clubb, A. Corsi, A. De Cia, J. A. de Diego, A. V. Filippenko, O. D. Fox, A. Gal-Yam, N. Gehrels, L. Georgiev, J. J. González, M. M. Kasliwal, P. L. Kelly, S. R. Kulkarni, A. S. Kutyrev, W. H. Lee, J. X. Prochaska, E. Ramirez-Ruiz, M. G. Richer, C. Román-Zúñiga, L. Singer, D. Stern, E. Troja, and S. Veilleux. Optical and Near-infrared Observations of SN 2013dx Associated with GRB 130702A. , 818(1): 79, Feb. 2016. doi: 10.3847/0004-637X/818/1/79.

[89] C. A. Tremonti, T. M. Heckman, G. Kauffmann, J. Brinchmann, S. Charlot, S. D. M. White, M. Seibert, E. W. Peng, D. J. Schlegel, A. Uomoto, M. Fukugita, and J. Brinkmann. The Origin of the Mass-Metallicity Relation: Insights from 53,000 Star-forming Galaxies in the Sloan Digital Sky Survey. , 613(2):898–913, Oct. 2004. doi: 10.1086/423264.

[90] S. Van Der Walt, S. C. Colbert, and G. Varoquaux. The numpy array: a structure for efficient numerical computation. *Computing in Science & Engineering*, 13(2):22, 2011.

[91] G. Van Rossum and F. L. Drake Jr. *Python tutorial*. Centrum voor Wiskunde en Informatica Amsterdam, The Netherlands, 1995.

[92] D. Watson, J. P. U. Fynbo, C. Ledoux, P. Vreeswijk, J. Hjorth, A. Smette, A. C. Andersen, K. Aoki, T. Augusteijn, A. P. Beardmore, D. Bersier, J. M. Castro Cerón, P. D'Avanzo, D. Diaz-Fraile, J. Gorosabel, P. Hirst, P. Jakobsson, B. L. Jensen, N. Kawai, G. Kosugi, P. Laursen, A. Levan, J. Masegosa, J. Näränen, K. L. Page, K. Pedersen, A. Pozanenko, J. N. Reeves, V. Rumyantsev, T. Shahbaz, D. Sharapov, J. Sollerman, R. L. C. Starling, N. Tanvir, K. Torstensson, and K. Wiersema. A $\log N_{HI}$ = 22.6 Damped Lyα Absorber in a Dark Gamma-Ray Burst: The Environment of GRB 050401. , 652(2):1011–1019, Dec. 2006. doi: 10.1086/508049.

[93] J. Wei, B. Cordier, S. Antier, P. Antilogus, J. L. Atteia, A. Bajat, S. Basa, V. Beckmann, M. G. Bernardini, S. Boissier, L. Bouchet, V. Burwitz, A. Claret, Z. G. Dai, F. Daigne, J. Deng, D. Dornic, H. Feng, T. Foglizzo, H. Gao, N. Gehrels, O. Godet, A. Goldwurm, F. Gonzalez, L. Gosset, D. Götz, C. Gouiffes, F. Grise, A. Gros, J. Guilet, X. Han, M. Huang, Y. F. Huang, M. Jouret, A. Klotz, O. La Marle, C. Lachaud, E. Le Floch, W. Lee, N. Leroy, L. X. Li, S. C. Li, Z. Li, E. W. Liang, H. Lyu, K. Mercier, G. Migliori, R. Mochkovitch, P. O'Brien, J. Osborne, J. Paul, E. Perinati, P. Petitjean, F. Piron, Y. Qiu, A. Rau, J. Rodriguez, S. Schanne, N. Tanvir, E. Vangioni, S. Vergani, F. Y. Wang, J. Wang, X. G. Wang, X. Y. Wang, A. Watson, N. Webb, J. J. Wei, R. Willingale, C. Wu, X. F. Wu, L. P. Xin, D. Xu, S. Yu, W. F. Yu, Y. W. Yu, B. Zhang, S. N. Zhang, Y. Zhang, and X. L. Zhou. The Deep and Transient Universe in the SVOM Era: New Challenges and Opportunities - Scientific prospects of the SVOM mission. *arXiv e-prints*, art. arXiv:1610.06892, Oct. 2016.

[94] S. E. Woosley and J. S. Bloom. The Supernova Gamma-Ray Burst Connection. , 44 (1):507–556, Sept. 2006. doi: 10.1146/annurev.astro.43.072103.150558.

[95] K. Yabe, K. Ohta, F. Iwamuro, S. Yuma, M. Akiyama, N. Tamura, M. Kimura, N. Takato, Y. Moritani, M. Sumiyoshi, T. Maihara, J. Silverman, G. Dalton, I. Lewis, D. Bonfield, H. Lee, E. Curtis Lake, E. Macaulay, and F. Clarke. NIR Spectroscopy of Star-Forming Galaxies at z 1.4 with Subaru/FMOS: The Mass-Metallicity Relation. , 64:60, June 2012. doi: 10.1093/pasj/64.3.60.

[96] H. J. Zahid, L. J. Kewley, and F. Bresolin. The Mass-Metallicity and Luminosity-Metallicity Relations from DEEP2 at z ~0.8. , 730(2):137, Apr. 2011. doi: 10.1088/0004-637X/730/2/137.

[97] H. J. Zahid, M. J. Geller, L. J. Kewley, H. S. Hwang, D. G. Fabricant, and M. J. Kurtz. The Chemical Evolution of Star-forming Galaxies over the Last 11 Billion Years. , 771(2):L19, July 2013. doi: 10.1088/2041-8205/771/2/L19.

APPENDIX

Permissions from the first authors of Tremonti et al. [89] and Sanders et al. [76] for use of their figures are shown below. Additionally shown is permission from *IOP Publishing*.

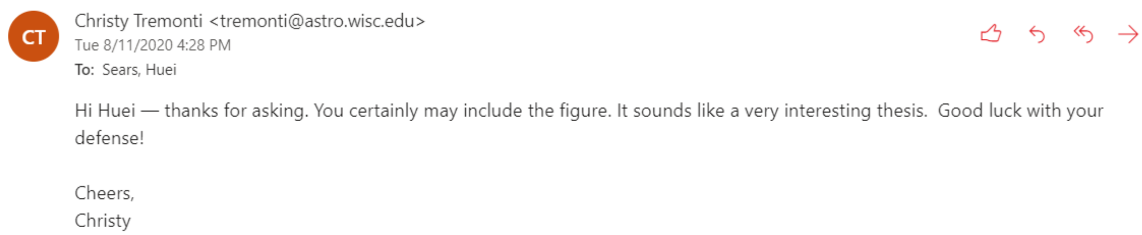

CT

Christy Tremonti <tremonti@astro.wisc.edu>
Tue 8/11/2020 4:28 PM
To: Sears, Huei

Hi Huei — thanks for asking. You certainly may include the figure. It sounds like a very interesting thesis. Good luck with your defense!

Cheers,
Christy

Figure A.1: A screenshot of e-mail communication with Dr. Christy Tremonti showing her approval for figure reproduction.

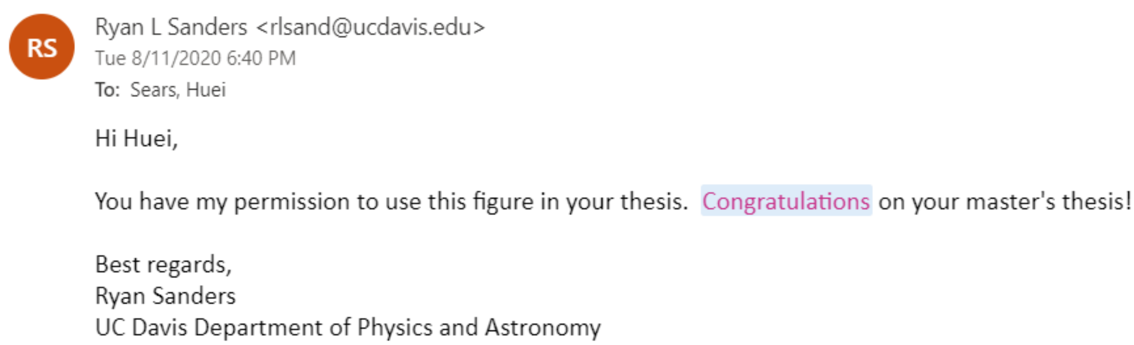

RS

Ryan L Sanders <rlsand@ucdavis.edu>
Tue 8/11/2020 6:40 PM
To: Sears, Huei

Hi Huei,

You have my permission to use this figure in your thesis. Congratulations on your master's thesis!

Best regards,
Ryan Sanders
UC Davis Department of Physics and Astronomy

Figure A.2: A screenshot of e-mail communication with Dr. Ryan Sanders showing his approval for figure reproduction.

P

Permissions <permissions@ioppublishing.org>
Thu 8/13/2020 9:22 AM
To: Sears, Huei

Dear Huei Sears,

Thank you for providing confirmation that you have received the consent of the authors to reproduce content from AAS journals ***(as below)***

I am happy to confirm that permission is granted and you need take no further action.

Please include the following alongside the material:

- the source of the material, including author, article title, title of journal, volume number, issue number (if relevant), page range (or first page if this is the only information available) and date of first publication. This material can be contained in a footnote or reference.
- for material being published electronically, a link back to the article (via DOI)
- if practical and IN ALL CASES for works published under any of the Creative Commons licences the words "© AAS. Reproduced with permission".

This permission does not apply to any material/figure which is credited to another source in the AAS publication or has been obtained from a third party. Express permission for such materials/figures must be obtained from the copyright owner.

Kind regards,

Cameron Wood

Figure A.3: A screenshot of e-mail communication with *IOP Publishing* showing their approval for figure reproduction.